Nature Sustainability, Volume 2, December 2019, pp. 1097–1105
DOI: 10.1038/s41893-019-0421-0

Viscoelastic Solid Repellent Coatings for Extreme Water-Saving and Global Sanitation

Jing Wang[†,‡], Lin Wang[‡,‖,], Nan Sun[†,‡,*], Ross Tierney[§], Hui Li[¶], Margo Corsetti[†], Leon Williams[§], Pak Kin Wong[†,¶] and Tak-Sing Wong[†,‡,¶,**]*

†Department of Mechanical Engineering, The Pennsylvania State University, University Park, PA 16802, USA

‡Materials Research Institute, The Pennsylvania State University, University Park, PA 16802, USA

‖ Department of Materials Science and Engineering, The Pennsylvania State University, University Park, PA 16802, USA

§Centre for Competitive Creative Design, Cranfield University, Bedfordshire, MK43 0AL, UK

¶ Department of Biomedical Engineering, The Pennsylvania State University, University Park, PA 16802, USA

*Equal contribution. **Corresponding author.

Word Count (including Abstract paragraph): 4152

Word Count (excluding Abstract paragraph): 3981

Word Count in Captions: 668

Number of Figures: 6

ABSTRACT

Water scarcity threatens over half of the world population, yet over 141 billion liters of fresh water is used globally each day for toilet flushing. This is nearly 6 times the daily water consumption of the population in Africa. The toilet water footprint is so large primarily because large volumes of water are necessary for the removal of human feces; human feces is viscoelastic and sticky in nature, causing it to adhere to conventional surfaces. Here, we designed and fabricated the liquid-entrenched smooth surface (LESS), a sprayable non-fouling coating that can reduce cleaning water consumption by ~90% compared to untreated surfaces due to its extreme repellency towards liquids, bacteria, and viscoelastic solids. Importantly, LESS-coated surfaces can repel viscoelastic solids with dynamic viscosities spanning over 9 orders of magnitude, i.e., three orders of magnitude higher than previously reported for other repellent materials. With an estimated >~1 billion toilets and urinals worldwide, incorporating LESS coating into sanitation systems will have significant implications for global sanitation and large-scale wastewater reduction for sustainable water management.

Water shortage is one of today's most pressing global issues[1]. In 2016, 4 billion people in the world faced severe water scarcity[2]. With the growing world population, fresh water supply continues to be in high demand with typical consumption ranging from everyday household to industrial activities[3]. To address the water shortage issue, mainstream research has been focused on finding new methods for sourcing fresh water such as water desalination and treatment[4-6], and techniques for harvesting water from air[7-10]. Methods for reducing water waste by minimizing wastewater generation from daily household and industrial activities, such as toilet flushing, have received relatively less attention.

In the United States, toilet flushing accounts for 24% of all indoor domestic wastewater-producing activities, and is the largest contributor of indoor household wastewater production[11]. Globally, it is estimated that over 141 billion liters of water – nearly 6 times the daily water consumption of the entire population in Africa[12] – is used each day for toilet flushing alone[13]. A number of approaches have been proposed to reduce fresh water consumption for toilet flushing that range from the use of rainwater for flushing[14] to the use of self-contained dry toilets[15]. Owing to a great variety of complex factors such as local environment[16], resource availability[17], and user preference[18], none of these approaches can completely address the water consumption issue. A relatively unexplored approach is to engineer the material interface of toilet surfaces to significantly weaken the adhesion of human feces and urine in order to reduce the amount of flushing water for waste removal.

Here, we report the design, fabrication, and performance as it relates to sanitation and water reduction of liquid-entrenched smooth surfaces (LESS), a sprayable, multifunctional surface coating that can reduce cleaning water consumption by ~90% compared to an uncoated surface. LESS is designed to repel aqueous fluids, bacteria, and viscoelastic solids with dynamic

viscosities spanning over 9 orders of magnitude (i.e., from ~10^{-3} Pa·s to ~10^{5} Pa·s) – three orders of magnitude higher than previously reported for other repellent materials. To our knowledge, no state-of-the-art liquid repellent surfaces have demonstrated repellency against viscoelastic solids with dynamic viscosity higher than ~100 Pa·s[19-26].

LESS consist of a nanoscopically smooth solid surface that is functionalized with molecularly-grafted polymers that stabilize a thin layer of lubricant through intermolecular forces. In addition, LESS can be applied onto various hydrophilic surfaces (e.g., ceramic, vitreous china, carbon steel, etc.) and complex geometries within minutes at ambient conditions. Additionally, we have shown that LESS can maintain non-stickiness toward human feces, outperforming other commercially available materials. We have further demonstrated that LESS possesses excellent anti-biofouling properties, which could reduce the use of aggressive chemicals currently used for sterilization. For a standard toilet using 1.6 gallons per flush (~ 6 liters per flush), our characterization and analysis show that every 1 milliliter of LESS coating fluid could have potential water-saving up to >1000 liters. Our coating is highly scalable and can be easily incorporated into used or existing ceramic- and metal-based toilets and urinals for improving global sanitation and reducing wastewater production, a challenge that is listed as one of the 17 Sustainable Development Goals by the United Nations (i.e., clean water and sanitation).

RESULTS AND DISCUSSION

Our LESS coatings are designed through interfacial adhesion and thermodynamic analyses to effectively repel liquid, bacteria, and viscoelastic solids, and have been characterized under relevant experimental conditions related to sanitation and water conservation applications.

Design criteria of LESS. Reducing the adhesion between viscoelastic solid and substrate surface would require lowering the work of adhesion, w_a. Specifically, the work of adhesion can be expressed as $w_a = R(\gamma_{13} + \gamma_{23} - \gamma_{12})$, which can be further simplified by Girifalco and Good equation[27] as $w_a = 2R(\gamma_{13} \bullet \gamma_{23})^{1/2}$ where R is surface roughness defined as the ratio between apparent and projected surface areas of the solid substrate, and γ_{ij} is the interfacial energy at the *i-j* interface, and 1, 2, and 3 refer to the solid substrate, the viscoelastic solid, and air, respectively. Therefore, minimizing w_a can be achieved 1) physically by reducing the surface roughness, R, and 2) chemically by reducing the interfacial energies of the underlying solid-air interface (γ_{13}) and the viscoelastic solid-air interface (γ_{23}) simultaneously.

Accordingly, we designed LESS based on the above physical and chemical criteria. To reduce w_a physically, a nanoscopically smooth solid substrate is used (i.e., $R \sim 1$) since the total work of adhesion between two surfaces is directly proportional to their respective contact area, which could be significantly increased by the presence of roughness[27]. Specifically, Dahlquist[28] showed experimentally that when the storage modulus of an adherent material is below a certain critical value (i.e., typically 0.3 MPa), the material will begin to flow and form conformal contact with the surface roughness of the adherent regardless of the applied pressure. Our adhesion measurements have further confirmed that surface adhesion of viscoelastic solids increases with the surface roughness (with average roughness, R_a ranges from 0.87±0.06 nm to 4.12±0.26 µm, Supplementary Note 1), indicating a relatively smooth surface is important in reducing surface adhesion with viscoelastic solids.

Reducing w_a chemically can be achieved conventionally by functionalizing a smooth solid substrate with a low surface energy coating (i.e., reduce γ_{13}), or by adding lubricant to be absorbed by viscoelastic solid[29] (i.e., reduce γ_{23}). To further reduce the w_a, both γ_{13} and γ_{23} can be

reduced simultaneously by creating a stable lubricant layer between the substrate and the viscoelastic solid (Supplementary Fig. 1a, Supplementary Note 2). Unlike wetting of a liquid film on rough solids[30,31], achieving super-wetting of a liquid film on smooth surface is more challenging and requires the use of intermolecular forces to stabilize the thin liquid film[24,32]. Thermodynamically, to achieve this condition the lubricant should have a non-negative spreading parameter S on the solid substrate and a positive disjoining pressure $\Pi(e)$[33-35] in the presence of both air and the foreign immiscible liquid of interest (i.e., $S \geq 0$ and $\Pi(e) > 0$), respectively (Methods).

Fabrication and characterization of LESS. Based on these design criteria, we have developed a number of LESS coatings for silica-based materials, such as glass, silicon, and china, etc. These substrates were chosen based on their inherent smoothness (with $R_a \sim 1$ nm) and their hydroxyl groups availability, which made surface functionalization facile[36]. We further functionalized these surfaces with dimethyldimethoxysilane to create polydimethylsiloxane (PDMS)-grafted chemical layer ($\gamma_{13} \approx 21$ mN/m^2). In addition, silicone oil was chosen as the lubricating fluid due to its strong chemical affinity towards the PDMS-grafted surfaces as well as its excellent chemical stability[37] and low environmental impact[38]. Furthermore, our calculations of spreading parameters and Hamaker constants have shown that this specific material combination (i.e., silicone oil and the PDMS-grafted surface) satisfies the requirement for a stable lubricant film formation (i.e., $S \geq 0$ and $A > 0$, Supplementary Note 3, Supplementary Tables 1 and 2), which are consistent with our experimental observations (Supplementary Video 1).

Our LESS can be formed on a range of substrates through a two-step spray coating process (Fig. 1, Supplementary Video 2). The first step generates a covalently-bonded chemical layer on

the substrate, and the second step creates an overcoat lubricant layer. Before the surface functionalization, the surfaces need to be rinsed with isopropanol and deionized water in order to remove surface contaminants and expose the hydroxyl groups. Once the surface is clean and dry, a solution containing dimethyldimethoxysilane is sprayed onto the surface at ambient conditions, allowing these molecules to react with the hydroxyl groups and forming a covalently-bonded PDMS-grafted layer on the substrate. After rinsing with isopropanol and ethanol to remove the excess PDMS, the silanized substrate then becomes hydrophobic and can repel both water and alkanes[26]. This step is modified from the method developed by Wang and McCarthy[26] without the need for oxygen plasma treatment, which allows for simpler and more scalable fabrication process. The formation of the new surface functional group was confirmed by X-ray photoelectron spectroscopy (XPS) measurements showing the formation of Si-O bonds associated with dimethyldimethoxysilane (Supplementary Fig. 2). The thickness of the PDMS-grafted layer was estimated to be ~1.3 nm from the XPS measurement[39] (Supplementary Note 4), and the water contact angle hysteresis of the surface is 6.8±0.5° (Supplementary Table 3). In the second step, the PDMS-grafted surface is preferentially wetted by silicone oil, forming a stable lubricating layer. The thickness of the lubricant can be controlled by either spin-coating or spray-coating. In our experiments, the typical thickness of the lubricant is controlled to be ~1 μm to ~10 μm.

Distinct from other fabrication methods to create liquid-infused slippery surfaces which generally take on the order of hours to complete[32,40-42], our two-step fabrication process takes less than ~5 minutes (Supplementary Video 2), and can be applied to other hydrophilic materials such as ceramic, carbon steel, titanium, etc. (Supplementary Video 3, Supplementary Table 4). LESS can effectively repel rain water, soapy water, and hard water (Supplementary Note 5,

Supplementary Fig. 3, Supplementary Tables 5 to 8), as well as synthetic feces (Fig. 2a, Methods, Supplementary Video 2) of dynamic viscosities spans over 9 orders of magnitude (i.e., from ~10^{-3} Pa·s to ~10^{5} Pa·s), as compared to other control surfaces including an uncoated surface, a superhydrophobic surface, a PDMS-grafted smooth surface, and a slippery liquid-infused porous surface (SLIPS)-coated surface (Fig. 2, Supplementary Video 4)[19-26]. Furthermore, we have demonstrated that our LESS coating can be applied onto complex geometries under room conditions without the use of advanced equipment. As a demonstration, we applied LESS coating onto a toilet bowl surface through a spray-coating process, where the coating can repel both dyed water and synthetic feces more effectively than those of a commercial hydrophobic glaze coated toilet (Fig. 3, Supplementary Videos 5 and 6).

Adhesion of LESS against viscoelastic synthetic feces. To quantify the anti-adhesion performance of LESS-coated surface, we performed surface adhesion measurements using synthetic feces against other control surfaces. We prepared synthetic feces with organic solid content similar to that of human feces[43] for adhesion characterization (Methods, Supplementary Tables 9 and 10). The solid contents of the synthetic feces range from 10 wt% to 60 wt%, which correspond to storage modulus of ~ 1 Pa (~10 wt%) to ~10^{5} Pa (~60 wt%) (Supplementary Fig. 4). These values closely emulate those of the fresh human feces[44,45].

First, we investigated the importance of a stable lubricant layer for reducing surface adhesion. The control surfaces in these tests include uncoated bare glass with and without lubrication of silicone oil, and PDMS-grafted glass. We normalized the work of debonding of the synthetic feces on lubricated surfaces (lubricated glass and LESS) by that of the uncoated bare glass. Our results showed that lubrication on bare glass can reduce the surface adhesion by ~41% for synthetic feces with 40% solid content (i.e., the stickiest sample in the test). In comparison,

grafted-PDMS glass can reduce the surface adhesion by ~75%, while the LESS coating can reduce the adhesion by ~90% (Supplementary Fig. 1b). These experimental results are consistent to the predictions of work of adhesion, showing up to 46% reduction on lubricated glass, 74% reduction on silanized glass, and 86% reduction on LESS-coated glass compared to untreated glass, respectively (Supplementary Note 2). Our results indicate that the presence of stable lubricating layer on the underlying solid substrate is critical to reduce surface adhesion.

In the second set of tests, we investigated the influence of underlying surface roughness of the lubricated substrates to the overall adhesion performance. The control surfaces in these tests include uncoated glass and silicone-oil infused SLIPS samples with either microscale (R_a ~ 4 μm) or nanoscale roughness (R_a < 1 μm) on the underlying substrates (Supplementary Note 1). Our measurements showed that the adhesion increases with increasing underlying surface roughness (Supplementary Fig. 5, Supplementary Table 4). In general, the LESS-coated surface outperforms other control surfaces, including uncoated surfaces with or without lubrication, and SLIPS with different underlying roughness. According to these tests (Fig. 4a), LESS coating can lead to 90% adhesion reduction in synthetic feces (~40% solid content, with viscoelastic characteristics similar to a Type 3 – 4 healthy human feces[44,45]) compared to those of the uncoated surfaces.

Water consumption of LESS. To investigate the amount of water that would be required to clean LESS after it is contaminated with the synthetic feces, we built a simplified open-channel experimental setup to emulate the toilet flushing process. Specifically, our setup is capable of generating a flow rate from 1 gallon per minute (i.e., 3.8 L/min with Reynolds number, *Re* ~ 4570, calculated based on the hydraulic diameter[46], Supplementary Note 6) up to 2.5 gallon per minute (i.e., ~9.5 L/min with *Re* ~ 11600). The estimated wall shear stresses generated by these

flows range from 0.093 Pa (at 1 gallon per min) up to 0.60 Pa (at 2.5 gallon per min), which are similar to those of typical toilets (i.e., ~0.11 Pa to ~0.78 Pa[47], Supplementary Note 6, Supplementary Table 11). To simulate the adhesion of feces to toilet surfaces during defecation, we dropped the synthetic feces (~5 grams) from a height of ~400 mm onto the test surfaces at a tilting angle of 45°. We then put the surfaces inside our open channel flow system to determine the amount of water required to completely remove the feces and their residues (Methods, Supplementary Fig. 6). We verified the complete removal of the feces residues using fluorescent trace dye, which was mixed with the synthetic feces during our tests (Supplementary Fig. 7). Compared to uncoated glass surfaces, LESS-coated surfaces reduce water consumption to clean the surface by up to 90% for various synthetic feces at different solid contents (Figs. 4b, c). We have also conducted similar characterizations on SLIPS samples and found that the water consumption increases with increasing underlying substrate roughness – a trend that is consistent with the observations in the adhesion tests (Supplementary Figs. 5 and 6).

Adhesion against human feces. We further compared the adhesion characteristics of human feces on LESS and other state-of-the-art commercially available surfaces (Figs. 5a, b, Supplementary Video 7). Specifically, we used glazed ceramic (a typical toilet material), Teflon, and silicone as the control surfaces. For these tests, we used a setup that allows human feces samples to be released from a drop rig at the same height onto an acrylic support where the test coating is placed. When the support pin for the acrylic surface is removed, the surface drops from a horizontal position to a vertical position, where the feces are expected to slide down the face of the surface. In our tests, all the commercial surfaces show extreme stickiness towards the human feces samples. LESS-coated glass, however, was the only surface showing non-stickiness towards the feces sample and left no noticeable residue behind (Fig. 5b). Furthermore, we have

shown in a different set of feces impact tests that traces of feces were left on a SLIPS-coated surface (with underlying surface roughness ~ 1 μm) (Supplementary Fig. 8). Therefore, our tests further demonstrate that the LESS coating outperforms various state-of-the-art surfaces on repelling human feces.

Anti-bacterial performance of LESS. One important reason that urinals or toilets need to be flushed and cleaned regularly is to prevent the growth of bacteria and spread of infectious diseases and odor generation. In certain regions (e.g., Brazil), rainwater is used as the source for toilet flushing. However, rainwater can contain bacteria that may contaminate the sanitation facilities[14]. Owing to the presence of the mobile lubricant interface of LESS, we hypothesize that LESS may have a strong anti-biofouling performance towards bacteria[23,48,49]. To verify this, we performed biofouling analyses on LESS-coated substrates using natural rainwater and bacteria-contaminated synthetic urine. Specifically, we collected rainwater from a house roof in State College, PA, USA, and measured its bacteria content and concentration (Methods). We identified the bacteria in the rainwater[50] using a MALDI Biotyper system (Fig. 5c, Supplementary Note 7, Supplementary Table 12). We rinsed the LESS-coated substrate and uncoated bare glass with the collected rainwater for 1 min, and then immediately incubated the substrates by attaching solid agar onto the surfaces in an incubator. After 36 hours of incubation, we counted the bacterial colonies on these surfaces. Specifically, no observable bacteria colonies were found on all LESS-coated substrates; whereas the untreated glass surfaces were contaminated with the bacteria in the rainwater (Fig. 5c).

In a different scenario, 10 mL of *Escherichia coli* (*E. Coli*) contaminated synthetic urine was sprayed onto the test surfaces, followed by the aforementioned procedures for the biofouling characterizations. Our test results are similar to those found in the rainwater tests, where all

LESS-coated samples showed no observable bacteria colonies while the glass substrate showed significant contamination with bacteria (Supplementary Fig. 9). We have further shown that LESS-coated substrates can repel all bacteria-contaminated synthetic urine with a sliding angle of a droplet (10 μL) less than 5^{o} (Supplementary Fig. 10). In the case when all lubricant is depleted, we have shown that LESS is much easier to be sterilized than other liquid-infused surfaces with underlying surface roughness (Supplementary Fig. 11).

In addition to rainwater and contaminated urine, we have also tested bacterial fouling on LESS-coated and untreated glass using synthetic fecal waste with different solid content percentage (10%, 30% and 50%) spiked with 10^8 cfu/ml *Escherichia coli* (Supplementary Fig. 12). Followed by the procedures described in Supplementary Note 8, we counted the bacteria colony number on these substrates after 24 hours incubation. Specifically, no visible bacteria colonies were found on LESS-coated substrate while up to ~2.5×10^5 colony/m^2 of bacteria colonies were observed on untreated glass (Fig. 5d, Supplementary Fig. 13).

All of these results indicate that LESS has excellent anti-biofouling performance and therefore could reduce the use of disinfectants or other aggressive chemicals currently used for cleaning and sterilization.

Durability of LESS. We have investigated the durability of the LESS coating against continuous shear flow, impact of synthetic feces, and mechanical abrasion. In the first test, we quantified the change of lubricant thickness by applying continuous shear flow with flow rates at 1 gallon/min and 2.5 gallon/min which correspond to shear stresses of ~0.1 Pa and ~0.6 Pa, respectively (Fig. 6a, Supplementary Table 11). Under these flow conditions, we have identified two regimes of lubricant depletion depending on the initial lubricant thickness. In the first regime

when the lubricant thickness is >>1 μm, the lubricant depletion rate is relatively high, and is typically on the order of ~0.01 μm/s. In the second regime when the lubricant thickness is <<1 μm, the lubricant depletion rate is significantly reduced to <<~0.01 μm/s. Note that a typical dual flush toilet consumes either 0.8 or 1.6 gallon per flush (gpf), and each flush takes on the order of 5 s[47]. Based on our experimental measurements, we estimate that our LESS coating with an initial thickness of ~1 μm can sustain >500 flushes in typical toilet environments.

In the second test, we have evaluated the lubricant durability using a water jet to simulate urination. It is known that the initial flow velocity of human urine ranges from 0.28 to 0.52 m/s[51]. Based on the Bernoulli's equation, we can estimate that the velocity of urine impacting on the surface is ~3 m/s (Methods, Supplementary Fig. 14). A water jet setup was built to achieve such an impact velocity. We designed each urination cycle to be consisted of a continuous flow of liquid jet for ~20 sec since it is reported that all mammals above 3 kg urinate for a constant time (~21±13 s) regardless of the size[52]. Contact angle hysteresis and thickness of the lubricant are measured after every 5 urination cycles. Our results showed that the LESS coating can withstand at least 50 urination cycles before further replenishment of the lubricant layer is necessary (Supplementary Fig. 15).

Furthermore, we tested the durability of the LESS coating by impacting synthetic feces of various solid contents, and we found that LESS coating can sustain ~10 to ~35 impact cycles (Fig. 6b, Supplementary Fig. 16). The loss of durability of our coating is mainly due to lubricant loss caused by feces adsorption at the point of contact. In addition, we have also characterized the robustness of our coating against mechanical abrasion. In our tests, we placed a mass of 0.5 kg onto a sandpaper (grit size: P400) and slid the sandpaper against the LESS-coated sample (Methods). Our results showed that the LESS coating can withstand at least ~300 abrasion cycles

before showing signs of degradation in liquid repellency performance (Fig. 6c).

We note that since the PDMS-grafted substrate of LESS is designed to adhere the silicone oil as opposed to aqueous liquids, it is possible to replenish the lubricant layer by incorporating small amounts of silicone oil in the flushing water so that the silicone oil can preferentially wet the surface through displacement wetting (Fig. 6d, Supplementary Note 9). Experimentally, we have shown that silicone oil wets the PDMS-grafted ceramic surface even when the surface has been pre-wetted by water, and subsequently forms a functional layer to repel the water (Fig. 6d, Supplementary Video 8).

Potential water-saving and environmental impact. To further estimate the potential water-saving of LESS coating on commercial toilets, we have conducted a minimal flush water test on a 1.6 gpf (or 6 Lpf) toilet to estimate the minimum water needed to flush the waste through the toilet trapway and drain line (Supplementary Note 10, Supplementary Fig. 17). In the test, we gradually reduced the water volume in the tank to flush the synthetic feces until they can no longer be completely flushed down the toilet. Our results showed that at least ~2.2±0.1 liters of flushing water are needed. This is equivalent to a potential water saving of up to ~63±2%. Using our experimental characterization results with ~1 mL of coating fluid to coat a toilet surface (~600 cm^2), it is estimated that one could save up to >1000 L of water for every mL of coating fluid used for a typical 1.6 gpf toilet. Furthermore, we estimated that the upper limit concentrations of the silicone oil in the flushed water to be on the order of ~0.03 parts per million (Supplementary Note 11). Recent studies have shown that silicone oil can be decomposed through various mechanisms in the environments[38]. More importantly, our LESS coating is not limited to grafted-PDMS and silicone oil system and can be formulated using natural oils as the lubrication layer.

SUMMARY

In summary, we have created a scalable, multifunctional LESS coating specifically designed to reduce adhesion to soft viscoelastic solids (e.g., human feces) with applications aimed to minimize water consumption for sanitation and waste management. We have shown that LESS coating is capable of reducing adhesion up to ~90% for soft viscoelastic solids and requires only ~10% of cleaning water required for an untreated control surface. The significant adhesion and water consumption reduction is due to the ability of the LESS coating to repel liquids, bacteria, and viscoelastic solids with dynamic viscosities spanning over 9 orders of magnitude. Our LESS coating can be applied onto various hydrophilic surfaces within minutes at ambient conditions through a spray coating process. Furthermore, the excellent anti-biofouling property of LESS could minimize the use of aggressive chemicals currently used for sterilization, thus reducing environmental impacts. Our analysis indicates that it is possible to save up to >1000 L of flushing water for every mL of coating fluid used for a standard 1.6 gpf toilet. Our coating can also be incorporated with novel waterless toilets to further enhance their function[53]. The ability to prevent fouling of fecal matter and bacteria will further reduce odor generation, which will make shared toilets more appealing to the public and could further promote safe and dignified sanitation. With an estimated > ~1 billion toilets and urinals around the world[13], it is anticipated that incorporating LESS coating into sanitation system worldwide could lead to significant water-saving and improved global sanitation, providing a key technological solution to one of the United Nations' Sustainable Development Goals in clean water and sanitation.

METHODS

Experimental details on the design and fabrication of the LESS coatings, preparation of synthetic feces, as well as the experimental characterizations and measurement procedures of the LESS coatings are presented below.

LESS coating solution preparation. The LESS coating can be prepared by first applying a PDMS-grafted layer onto a substrate followed by the addition of a lubricant. Specifically, the PDMS-grafted layer was prepared by spraying a silane solution onto a clean and dry hydrophilic substrate (e.g., glass or ceramic) using a modified process reported in [26]. The key ingredients of the silane solution are comprised of dimethyldimethoxysilane and small amount of sulfuric acid (Sigma Aldrich). The silicone oil (with a viscosity of 20 cSt, chemical formula: $(–Si(CH_3)_2O–)_n$) was used as the lubricant.

Synthetic feces preparation. The recipe of synthetic human feces was developed from the original recipe developed at the University of KwaZulu Natal at South Africa. The synthetic human feces are composed of yeast, psyllium, peanut oil, miso, polyethylene glycol, calcium phosphate, cellulose, and water. All solid components are expressed as dry mass, and the corresponding percentages are shown in Supplementary Table 9. The compositions of the synthetic feces are biologically very similar to human feces[43] (Supplementary Table 10). Note that human feces can be classified into 7 categories based on their solid content percentage and viscosities[54]. This specific classification, known as Bristol stool scale, ranges from Type 1 (hard solids) to Type 7 (entirely liquid). The viscosity of the synthetic feces can be tuned by the percentage of solid contents. We made synthetic feces with solid percentage of 10%, 20%, 30%, 40%, 50%, and 60%. Note that synthetic feces with ~40% solid content have viscoelastic

characteristics similar to a Type 3 – 4 healthy human feces. These synthetic feces were used within 5 hours of preparation for viscoelasticity measurements, adhesion tests, and water consumption tests.

Spreading parameter and Hamaker constant. We define the spreading parameters of the lubricant on the solid substrate in the presence of air as S_{ls} and that in the presence of the foreign immiscible fluid droplet as S_{lsf}, respectively. Specifically, these spreading parameters can be expressed as $S_{ls} = \sigma_s - (\sigma_{ls} + \sigma_l)$ and $S_{lsf} = \sigma_{sf} - (\sigma_{ls} + \sigma_{lf})$, where σ_s, σ_{ls}, σ_l, σ_{sf}, and σ_{lf} are the interfacial tensions of solid-air, lubricant-solid, lubricant-air, solid-immiscible fluid, and lubricant-immiscible fluid interfaces, respectively. In addition, the disjoining pressure of the lubricant film can be expressed as $\Pi(e) = A/6\pi e^3$, where e is the lubricant film height, and A is the Hamaker constant expressed as[27]:

$$A = \frac{3}{4}kT\left(\frac{\varepsilon_s - \varepsilon_l}{\varepsilon_s + \varepsilon_l}\right)\left(\frac{\varepsilon_f - \varepsilon_l}{\varepsilon_f + \varepsilon_l}\right) + \frac{3h\nu_e}{8\sqrt{2}} \frac{\left(n_s^2 - n_l^2\right)\left(n_f^2 - n_l^2\right)}{\left(n_s^2 + n_l^2\right)^{1/2}\left(n_f^2 + n_l^2\right)^{1/2}\left[\left(n_s^2 + n_l^2\right)^{1/2} + \left(n_f^2 + n_l^2\right)^{1/2}\right]}$$

where k is the Boltzmann constant, T is the absolute temperature, h is the Planck's constant, and $\nu_e \sim 4\times10^{15}$ s^{-1} is the plasma frequency of free electron gas, while $\epsilon_{s/l/f}$ and $n_{s/l/f}$ are the dielectric constants and refractive indices of the solid, lubricant, and immiscible fluid of interest (air or water in our case), respectively.

Viscoelasticity and adhesion measurement. The viscoelasticity of synthetic human feces with different solid content percentage (10%, 20%, 30%, 40%, 50%, and 60%) was measured using a rheometer (DHR2, TA instrument). The adhesion measurement was performed using the rheometer by recording the axial force and displacement distance. The measurement consists of

three steps including compression, contact, and debonding from the synthetic feces: I) Compression: the synthetic feces were first preloaded on the test stage with a sample testing area of 25 mm × 25 mm. The axial force was kept below 110% of average feces impact force. To measure the average impact force of the feces, we dropped a piece of synthetic feces with certain weight (~5 grams) from 400 mm height and used a high-speed camera (Phantom Miro M320S) to measure the impact time. Transparent Cartesian graph papers were used to measure the corresponding impact area (Supplementary Table 13); II) Contact: After compressing the feces samples, the test probe remained in contact with the feces for 5 min before the debonding step; III) Debonding: The probe surface was pulled away at a constant velocity of 10 μm/s. The work of debonding was calculated as the integral of the axial force and distance. More than 5 independent measurements were performed for each adhesion measurement.

Water consumption measurement. To measure the water consumption to clean the surfaces after feces impact, a custom open channel flow system was built, which consisted of a water tank (McMaster-Carr), ½ inch inner diameter soft tubes, a valve and a pump (PMP-450S) (Koolance), a flowmeter (McMaster-Carr) with a range of 3.5 gallon/min, and a rectangle tube (2 inch × 2 inch) (McMaster-Carr). The flow rate was manually controlled with the valve, the pump, and the flowmeter.

Human fecal waste test. An 8-mm thick Teflon sheet (Direct Plastics) was cut into a tile of 80 mm × 80 mm. A silicone sheet (Silicon Engineering) with a hardness of shore 40A was cut into 80 mm × 80 mm. Ceramic used in the experiment was a gloss ceramic glazed bathroom tile purchased from a hardware store. The human feces were all donated anonymously from three different people. All three stool samples were between Type 3 and 5 according to the Bristol

Stool Scale (BSS), indicating that the samples have solid content between 15 wt% to 40 wt%. Human feces rated Type 3 – 5 on the BSS system is considered normal for a healthy adult.

Bacteria preparation and culture. The rainwater was collected from the roof of a house in State College, PA, and then stored in a refrigerator at 4 ^{o}C. We tested the concentration of bacteria in rainwater by diluting the rainwater by 10× with sterilized DI water, and spread 10 µL of the rainwater and the diluted solution on a solid agar. After culturing these samples in 37 ^{o}C incubator for 36 hours, we counted the number of bacterial colonies on the agar surface to determine the concentrations. We identified the bacteria in the rainwater using a MALDI Biotyper system; and these bacteria were identified as *Staphylococcus aureus*, *Enterobacter cloacae*, *Escherichia vulneris*, *Escherichia hermannii*, *Acinetobacter calcoaceticus*, *Enterococcus mundtii*, which are commonly found in rainwater. The *E. coli* 137 was collected from an infected urine sample with approval from Stanford University Institutional Review Board (IRB) and Veterans Affairs Palo Alto Health Care System (VAPAHCS) Research and Development committee. After liquid agar culturing, we diluted the bacteria sample with synthetic urine (Fisher Scientific) to a concentration representative of a urinary tract infection urine sample.

Durability tests. 1. Shear flow test: To test the durability of the LESS-coated surfaces under shear flow, we put LESS-coated glass under different shear flow conditions for 1 hour (i.e., at shear stresses of 0.1 Pa and 0.6 Pa at 1 gpm and 2.5 gpm, respectively). The corresponding lubricant loss was measured in every 5 minute-interval, which corresponds to ~60 toilet flushes as a typical toilet flush takes approximately 5 seconds. **2. Simulated urination test:** The LESS-coated surface was placed vertically (parallel to gravity), and the water jet impacted on the surface at ~45^{o} in the same spot during the test (see Supplementary Fig. 14). The

height (h) between the water level to the impacting point is ~450 mm, and the flow diameter (D) is ~6 mm. **3. Synthetic feces dropping and flushing test:** ~5 grams of synthetic human feces were dropped from 400 mm height onto the surface at a tilting angle of 45°. Then the LESS-coated surface was put into the flow system for cleaning at a flow rate of 1 gallon/min. Before and after the impact-and-flushing cycle, we measured the sliding angle of the surface using a 10 μL water drop (Supplementary Fig. 16). The LESS-coated surface was considered to be fully degraded if the sliding angle was >65°. **4. Abrasion test**. To test the robustness of the LESS-coated surfaces, we abraded the sample (area: 75 mm × 25 mm) with sandpaper (P400: average particle diameter of 35 μm) under a normal force of ~ 5 N. The sample was pulled in ~ 0.1 m/s for ~ 0.1 m per cycle. We measured the sliding angle of a 10 μL water drop on the sample for every 10 cycles. The performance of the LESS-coated surface was considered to be degraded when the sliding angle dramatically increases in tens of cycles. In our test, we observed that the sliding angle starts to increase after ~300 cycles.

ACKNOWLEDGEMENTS

We thank Vincent Bojan and Jeff Shallenberger at the Materials Research Institute of The Pennsylvania State University for the help with XPS measurement and data processing, Luke Andersson for the help with longevity test, Birgitt Boschitsch Stogin for the help with manuscript preparation, and Antonino Turrigiano for discussion. We thank Dr. Tatiana Laremore, director of the Huck Institutes of the Life Sciences Proteomics and Mass Spectrometry Core Facility for assistance with the MALDI Biotyper microorganism identification. We thank Prof. Joseph C. Liao from Stanford University for providing the urine sample. We acknowledge funding support by the National Science Foundation (CAREER Award# 1351462; I-Corps# 1757165, 1735627), the Wormley Family Early Career Professorship, and the Humanitarian Materials Initiative Award sponsored by Covestro and the Materials Research Institute at The Pennsylvania State University. Part of the work was conducted at the Penn State node of the NSF-funded National Nanotechnology of Infrastructure Network.

Data Availability

The authors declare that the data supporting the findings of this study are available within the paper and its Supplementary Information files. Additional data that support the findings of this study are available from the corresponding author upon request.

References

1 Eliasson, J. The rising pressure of global water shortages. *Nature* **517**, 6-7 (2015).

2 Mekonnen, M. M. & Hoekstra, A. Y. Four billion people facing severe water scarcity. *Science Advances* **2**, e1500323 (2016).

3 Attari, S. Z. Perceptions of water use. *Proceedings of the National Academy of Sciences* **111**, 5129-5134 (2014).

4 Shannon, M. A. *et al.* Science and technology for water purification in the coming decades. *Nature* **452**, 301-310 (2008).

5 Surwade, S. P. *et al.* Water desalination using nanoporous single-layer graphene. *Nature Nanotechnology* **10**, 459-464 (2015).

6 Chiavazzo, E., Morciano, M., Viglino, F., Fasano, M. & Asinari, P. Passive solar high-yield seawater desalination by modular and low-cost distillation. *Nature Sustainability* **1**, 763-772 (2018).

7 Parker, A. R. & Lawrence, C. R. Water capture by a desert beetle. *Nature* **414**, 33 (2001).

8 Ju, J. *et al.* A multi-structural and multi-functional integrated fog collection system in cactus. *Nature Communications* **3**, 1247 (2012).

9 Park, K.-C. *et al.* Condensation on slippery asymmetric bumps. *Nature* **531**, 78-82 (2016).

10 Kim, H. *et al.* Water harvesting from air with metal-organic frameworks powered by natural sunlight. *Science* **356**, 430-434 (2017).

11 DeOreo, W. B., Mayer, P. W., Dziegielewski, B. & Kiefer, J. *Residential end uses of water, version 2*. (Water Research Foundation, 2016).

12 United Nations Development Programme. *Human Development Report*. (UNDP, 2006).

13 World Health Organization and UNICEF. *Progress on sanitation and drinking water–2015 update and MDG assessment*. (World Health Organization, 2015).

14 Ghisi, E. & Ferreira, D. F. Potential for potable water savings by using rainwater and greywater in a multi-storey residential building in southern Brazil. *Building and Environment* **42**, 2512-2522 (2007).

15 WWAP (United Nations World Water Assessment Programme). The United Nations World Water Development Report 2016: Water and Jobs. *Paris, UNESCO* (2016).

16 Mahdavinejad, M., Bemanian, M., Farahani, S. F. & Tajik, A. Role of toilet type in transmission of infections. *Academic Research International* **1**, 110 (2011).

17 Paterson, C., Mara, D. & Curtis, T. Pro-poor sanitation technologies. *Geoforum* **38**, 901-907 (2007).

18 Lin, J. *et al.* Qualitative and quantitative analysis of volatile constituents from latrines. *Environmental Science & Technology* **47**, 7876-7882 (2013).

19 Tuteja, A. *et al.* Designing Superoleophobic Surfaces. *Science* **318**, 1618-1622 (2007).

20 Tuteja, A., Choi, W., Mabry, J. M., McKinley, G. H. & Cohen, R. E. Robust omniphobic surfaces. *Proc. Natl. Acad. Sci. U. S. A.* **105**, 18200-18205 (2008).

21 Liu, T. L. & Kim, C.-J. C. Turning a surface superrepellent even to completely wetting liquids. *Science* **346**, 1096-1100 (2014).

22 Wong, T.-S. *et al.* Bioinspired self-repairing slippery surfaces with pressure-stable omniphobicity. *Nature* **477**, 443 (2011).

23 Epstein, A. K., Wong, T.-S., Belisle, R. A., Boggs, E. M. & Aizenberg, J. Liquid-infused structured surfaces with exceptional anti-biofouling performance. *Proceedings of the National Academy of Sciences* **109**, 13182-13187 (2012).

24 Leslie, D. C. *et al.* A bioinspired omniphobic surface coating on medical devices prevents thrombosis and biofouling. *Nature Biotechnology* **32**, 1134-1140 (2014).

25 Wang, J., Kato, K., Blois, A. P. & Wong, T.-S. Bioinspired Omniphobic Coatings with a Thermal Self-Repair Function on Industrial Materials. *ACS Applied Materials & Interfaces* **8**, 8265-8271 (2016).

26 Wang, L. & McCarthy, T. J. Covalently attached liquids: instant omniphobic surfaces with unprecedented repellency. *Angewandte Chemie* **128**, 252-256 (2016).

27 Israelachvili, J. N. *Intermolecular and surface forces*. (Academic press, 2011).

28 Dahlquist, C. A. Pressure-sensitive adhesives. *Treatise on adhesion and adhesives* **2**, 219-260 (1969).

29 Gent, A. & Schultz, J. Effect of wetting liquids on the strength of adhesion of viscoelastic material. *The Journal of Adhesion* **3**, 281-294 (1972).

30 Wenzel, R. N. Resistance of solid surfaces to wetting by water. *Industrial & Engineering Chemistry* **28**, 988-994 (1936).

31 Drelich, J. & Chibowski, E. Superhydrophilic and superwetting surfaces: definition and mechanisms of

control. *Langmuir* **26**, 18621-18623 (2010).
32 Tenjimbayashi, M. *et al.* Liquid‐Infused Smooth Coating with Transparency, Super‐Durability, and Extraordinary Hydrophobicity. *Advanced Functional Materials* **26**, 6693-6702 (2016).
33 Daniel, D., Timonen, J. V., Li, R., Velling, S. J. & Aizenberg, J. Oleoplaning droplets on lubricated surfaces. *Nature Physics* **13**, 1020-1025 (2017).
34 De Gennes, P.-G., Brochard-Wyart, F. & Quéré, D. *Capillarity and wetting phenomena: drops, bubbles, pearls, waves*. (Springer Science & Business Media, 2013).
35 Preston, D. J., Song, Y., Lu, Z., Antao, D. S. & Wang, E. N. Design of Lubricant Infused Surfaces. *ACS Applied Materials & Interfaces* **9**, 42383-42392 (2017).
36 Zhuravlev, L. Concentration of hydroxyl groups on the surface of amorphous silicas. *Langmuir* **3**, 316-318 (1987).
37 Crisp, A., de Juan, E. & Tiedeman, J. Effect of silicone oil viscosity on emulsification. *Archives of Ophthalmology* **105**, 546-550 (1987).
38 Graiver, D., Farminer, K. & Narayan, R. A review of the fate and effects of silicones in the environment. *Journal of Polymers and the Environment* **11**, 129-136 (2003).
39 Seah, M. P. An accurate and simple universal curve for the energy-dependent electron inelastic mean free path. *Surface and Interface Analysis* **44**, 497-503 (2012).
40 Liu, H., Zhang, P., Liu, M., Wang, S. & Jiang, L. Organogel‐based Thin Films for Self‐Cleaning on Various Surfaces. *Advanced Materials* **25**, 4477-4481 (2013).
41 Zhang, C., Xia, Y., Zhang, H. & Zacharia, N. S. Surface Functionalization for a Nontextured Liquid-Infused Surface with Enhanced Lifetime. *ACS Applied Materials & Interfaces* **10**, 5892-5901 (2018).
42 Urata, C., Cheng, D. F., Masheder, B. & Hozumi, A. Smooth, transparent and nonperfluorinated surfaces exhibiting unusual contact angle behavior toward organic liquids. *RSC Advances* **2**, 9805-9808 (2012).
43 Rose, C., Parker, A., Jefferson, B. & Cartmell, E. The characterization of feces and urine: a review of the literature to inform advanced treatment technology. *Critical Reviews in Environmental Science and Technology* **45**, 1827-1879 (2015).
44 Woolley, S., Cottingham, R., Pocock, J. & Buckley, C. Shear rheological properties of fresh human faeces with different moisture content. *Water SA* **40**, 273-276 (2014).
45 Woolley, S., Buckley, C., Pocock, J. & Foutch, G. Rheological modelling of fresh human faeces. *Journal of Water Sanitation and Hygiene for Development* **4**, 484-489 (2014).
46 Yunus, A. C. & Cimbala, J. M. Fluid mechanics fundamentals and applications. *International Edition, McGraw Hill Publication* (2006).
47 Vickers, A. Water-use efficiency standards for plumbing fixtures: benefits of national legislation. *Journal (American Water Works Association)* **82**, 51-54 (1990).
48 Awad, T. S., Asker, D. & Hatton, B. D. Food-safe modification of stainless steel food processing surfaces to reduce bacterial biofilms. *ACS Applied Materials & Interfaces* **10**, 22902-22912 (2018).
49 Halvey Alex, K., Macdonald, B., Dhyani, A. & Tuteja, A. Design of surfaces for controlling hard and soft fouling. *Philosophical Transactions of the Royal Society A: Mathematical, Physical and Engineering Sciences* **377**, 20180266 (2019).
50 Evans, C., Coombes, P. J. & Dunstan, R. Wind, rain and bacteria: The effect of weather on the microbial composition of roof-harvested rainwater. *Water Research* **40**, 37-44 (2006).
51 Segura, C. G. Urine flow in childhood: a study of flow chart parameters based on 1,361 uroflowmetry tests. *The Journal of urology* **157**, 1426-1428 (1997).
52 Yang, P. J., Pham, J., Choo, J. & Hu, D. L. Duration of urination does not change with body size. *Proceedings of the National Academy of Sciences* **111**, 11932-11937 (2014).
53 Hennigs, J. *et al.* Field testing of a prototype mechanical dry toilet flush. *Science of the Total Environment* **668**, 419-431 (2019).
54 Lewis, S. & Heaton, K. Stool form scale as a useful guide to intestinal transit time. *Scandinavian Journal of Gastroenterology* **32**, 920-924 (1997).

AUTHOR INFORMATION

These authors contributed equally: Lin Wang and Nan Sun.

AUTHOR CONTRIBUTIONS

J.W. and T.S.W. designed the overall experiments. J.W. designed the LESS coating. J.W. and L.W. (Lin Wang) fabricated the LESS coating. J.W. and N.S. designed the adhesion tests. J.W., N.S., and M.C. performed the adhesion tests. J.W., L.W. (Lin Wang), H.L. and P.K.W. designed the anti-biofouling tests. J.W., L.W. (Lin Wang), and H.L. performed the anti-biofouling tests. R.T. and L.W. (Leon Williams) designed and performed the human feces tests. J.W. and L.W. (Lin Wang) designed and performed the durability tests. J.W., L.W. (Lin Wang), N.S., M.C., H. L., R.T., and T.S.W. analysed and processed the data. J.W. and T.S.W. wrote the manuscript. All authors reviewed the manuscript.

CORRESPONDING AUTHOR

Correspondence and requests for materials should be addressed to Tak-Sing Wong.

COMPETING INTERESTS

J.W. and T.-S.W. are the inventors on a patent application (PCT/US2017/062206) submitted by the Penn State Research Foundation that describes the LESS coating technology. T.-S.W. is a co-founder of the start-up company spotLESS Materials Inc. which commercializes the LESS coating technology.

ADDITIONAL INFORMATION

Supplementary information is available for this paper at https://doi.org/.

Reprints and permissions information is available at www.nature.com/reprints.

Correspondence and requests for materials should be addressed to T.S.W.

Publisher's note: Springer Nature remains neutral with regard to jurisdictional claims in published maps and institutional affiliations.

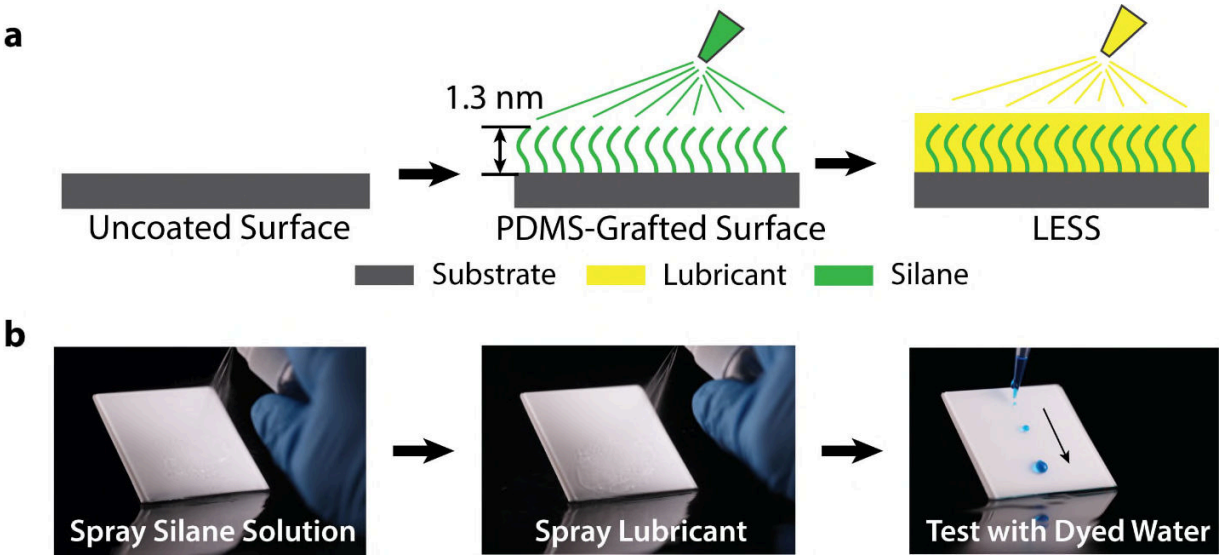

Figure 1. Fabrication of liquid-entrenched smooth surfaces (LESS). a, Schematic illustration showing a two-step spray coating process to form the LESS coating. The molecularly-grafted polymer layer creates chemical affinity to the lubricant. **b,** Optical images showing the individual coating processes on glass. The lubricant used was silicone oil and the blue testing liquid was dyed water.

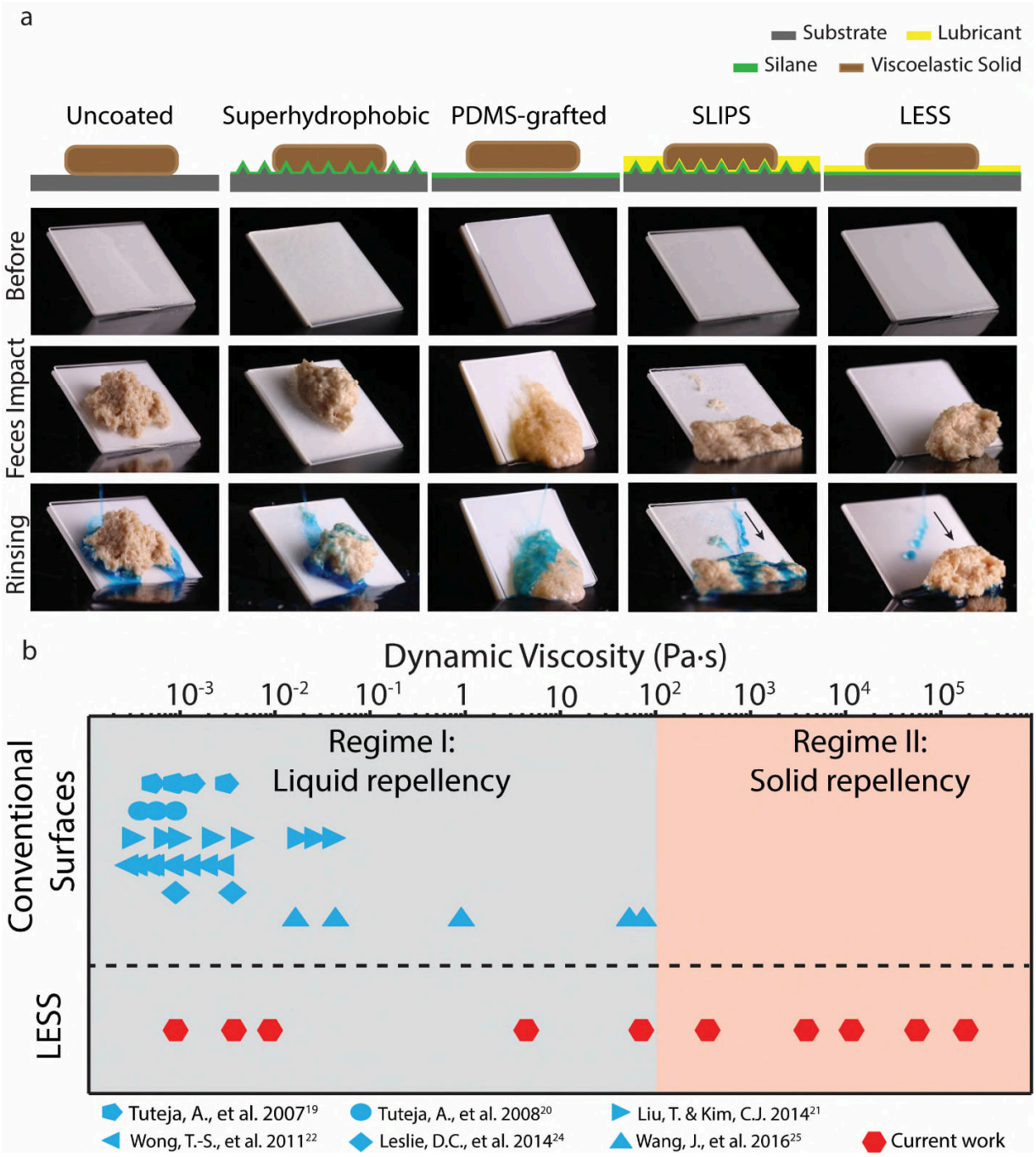

Figure 2. Overview of state-of-the-art liquid and viscoelastic solid repellent surfaces. a, Schematic and optical images showing the comparison of adhesion between viscoelastic solids and different engineered surfaces including (left to right) an uncoated glass, a superhydrophobic glass, a PDMS-grafted glass, a SLIPS-coated glass, and a LESS-coated glass. The

superhydrophobic glass was created using a commercially available superhydrophobic coating (NeverWet LLC). The SLIPS-coated glass has an underlying surface roughness ~1 μm. Synthetic feces with a solid content percentage of 30% (dynamic viscosity = ~2406 Pa·s) were used in these experiments. **b**, A plot showing the reported dynamic viscosity range of liquids and viscoelastic solids that can be repelled by the state-of-the-art liquid repellent surfaces and the LESS-coated surface.

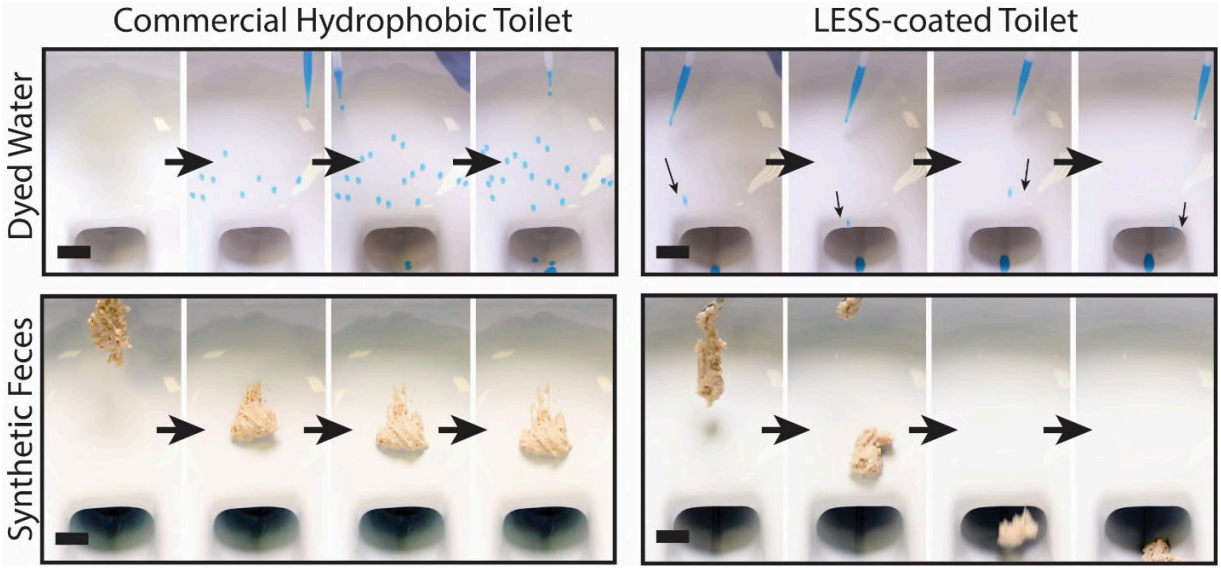

Figure 3. Comparison of liquid and synthetic feces repellency between a state-of-the-art commercial hydrophobic glaze coated toilet (SloanTec® hydrophobic glaze) and a LESS-coated toilet. Dyed water and synthetic feces at 30% solid content were used in these tests. The scale bar is 5 cm. See also Supplementary Videos 5 and 6 for details.

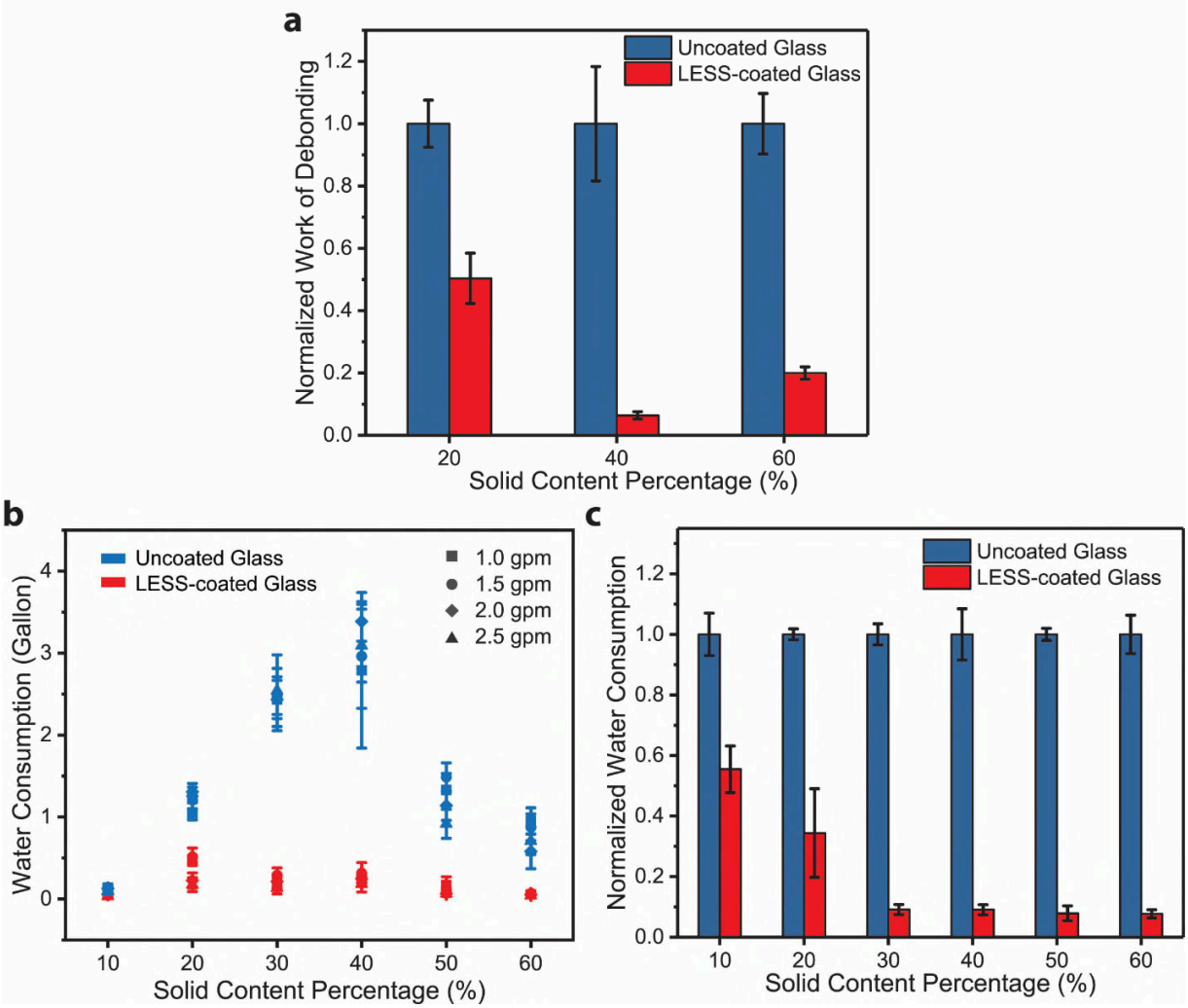

Figure 4. Work of adhesion and water consumption characterizations. a, Work of debonding of synthetic feces of varying solid contents on uncoated bare glass and LESS-coated glass. The data is normalized by the work of debonding of the synthetic feces on uncoated glass. **b,** Water consumption measurements on uncoated and LESS-coated glass under different flow rates after being impacted by ~5 grams of synthetic feces with different solid content percentage. Error bars represent standard deviations of four independent measurements. **c,** Cleaning water consumption performance of different surfaces after synthetic feces impact. The data is normalized by the

cleaning water consumption on uncoated glass with each solid weight percentage of synthetic feces. All error bars represent standard deviations of four to six independent measurements.

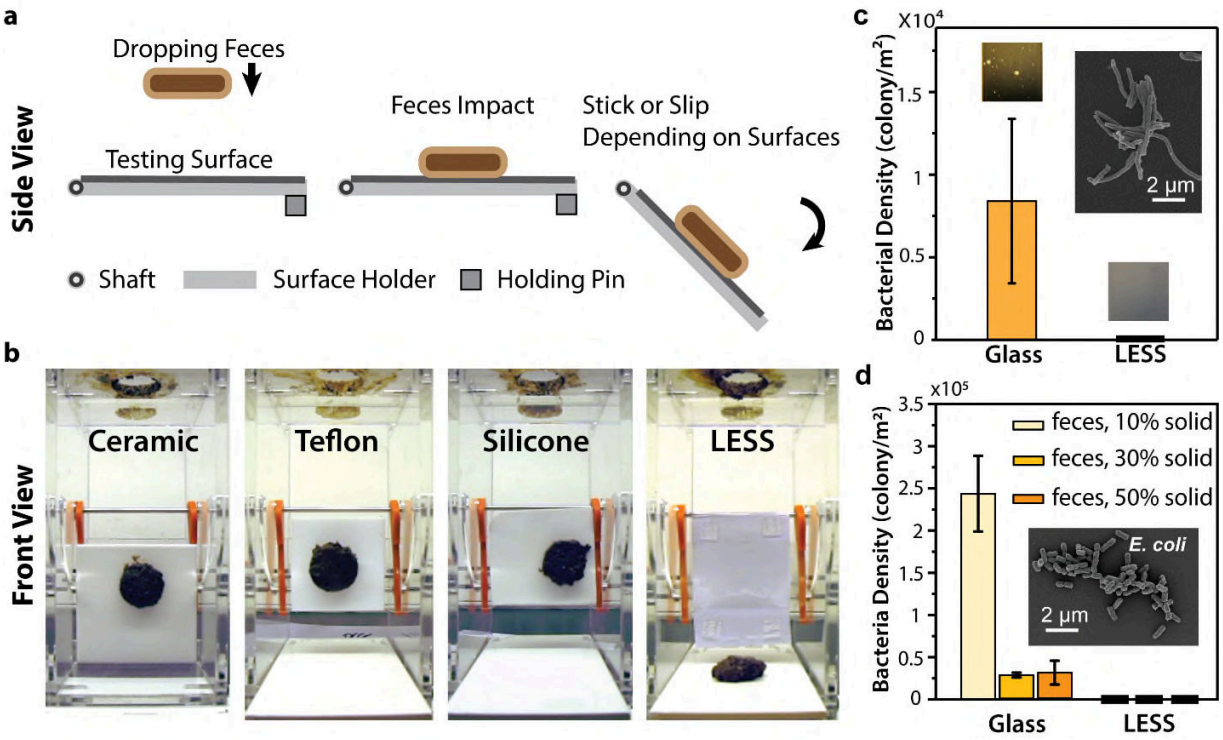

Figure 5. Anti-fouling performance of LESS. a, b, Human feces dropping test on commercially available surfaces and a LESS-coated surface. **a,** Schematic showing the human feces dropping test procedures: I) feces dropping from a height of 75 mm, II) feces impacting onto the test surfaces, and III) releasing the surface from horizontal to vertical to determine if feces will adhere onto the surface or not. **b,** Optical images showing the test results for different surfaces. The human feces adhere onto ceramic, Teflon, and silicone, but slide off from the LESS-coated glass. **c, d,** Anti-bacterial performance comparison. **c,** Bacteria adhesion test with rainwater on glass (control) and LESS-coated glass. Scanning electron microscope (SEM) images show two types of bacteria found in the rainwater sample. **d,** Bacteria adhesion test with *Escherichia coli* spiked synthetic feces (10%, 30%, and 50% solid content) on different surfaces. The inset image shows an SEM image of *E. coli*. Error bars in **c** and **d** represent standard deviations of three independent measurements.

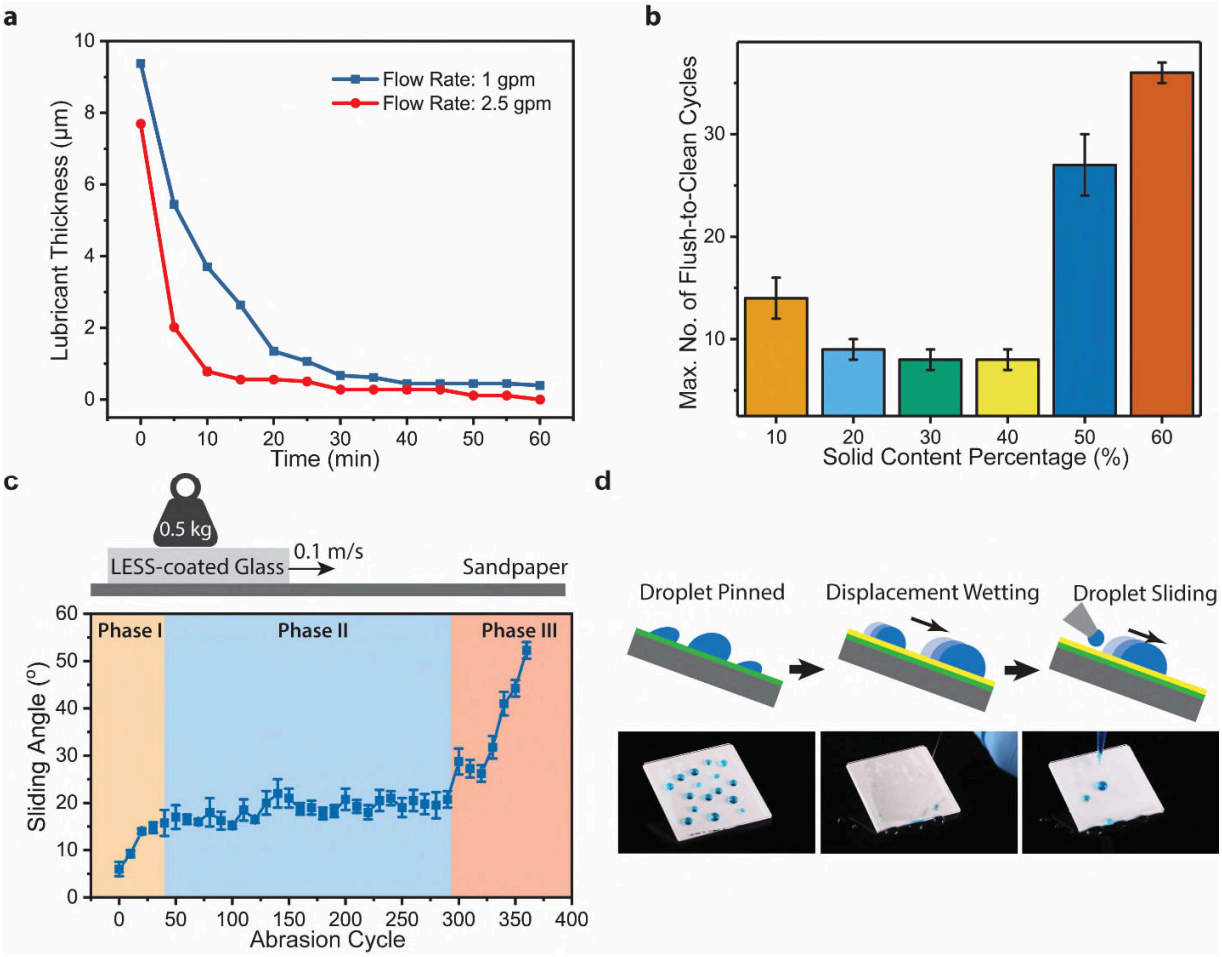

Figure 6. Durability characterizations and lubricant replenishment of LESS-coated surfaces. a, Durability of the lubricant layer (silicone oil with a viscosity of 20 cSt) under different shear flow conditions. Weight difference between LESS-coated and non-lubricated surface was measured and used to estimate the lubricant thickness. **b,** Durability of the LESS coating under continuous feces impact-and-flushing cycles. Error bars represent standard deviations of three independent measurements. **c,** Abrasion characterization on LESS-coated glass. Phase I indicates excess lubricant was removed from the LESS-coated substrate. Phase II indicates that the thickness of the lubricant reaches equilibrium with consistent liquid repellency

performance for up to ~300 abrasion cycle. Phase III indicates gradual degradation of the coating and small particles accumulation from the sandpaper scratches begin to induce droplet pinning. Error bars represent standard deviations of three independent measurements. **d,** Schematic showing the displacement wetting phenomenon on a PDMS-grafted glass. Optical images showing a facile lubricant replenishment process.

Nature Sustainability, Volume 2, December 2019, pp. 1097–1105
DOI: 10.1038/s41893-019-0421-0

Viscoelastic Solid Repellent Coatings for Extreme Water-Saving and Global Sanitation

Jing Wang[†,‡], Lin Wang[‡,‖,*], Nan Sun[†,‡,*], Ross Tierney[§], Hui Li[¶], Margo Corsetti[†], Leon Williams[§], Pak Kin Wong[†,¶] and Tak-Sing Wong[†,‡,¶,**]

[†]Department of Mechanical Engineering, The Pennsylvania State University, University Park, PA 16802, USA

[‡]Materials Research Institute, The Pennsylvania State University, University Park, PA 16802, USA

[‖]Department of Materials Science and Engineering, The Pennsylvania State University, University Park, PA 16802, USA

[§]Centre for Competitive Creative Design, Cranfield University, Bedfordshire, MK43 0AL, UK

[¶]Department of Biomedical Engineering, The Pennsylvania State University, University Park, PA 16802, USA

*Equal contribution.

**Corresponding author: T.S.W. (tswong@psu.edu).

Captions of Supplementary Videos

Supplementary Video 1 shows the super-wetting of silicone oil (20 cSt) on a PDMS-grafted glass surface. A 10 μL droplet of silicone oil was released onto a PDMS-grafted surface, which spread and completely wet the surface. Then 10 μL of water was put on the lubricated surface. The mobility of the water droplet indicates the formation of a stabilized silicone oil film.

Supplementary Video 2 shows the spray coating process to form LESS coating. The substrate used in the video was glass, and was cleaned by isopropanol, ethanol, and deionized water. We first sprayed ~2 mL of silane solution onto the glass surface, and let the surface dry for 3 min. Then silicone oil (with a viscosity of 20 cSt) was sprayed onto the surface. The LESS coating was then successfully formed by testing the surface with blue dyed water and synthetic feces at 20 wt% solid content. Both water and synthetic feces slide off the LESS-coated surface.

Supplementary Video 3 shows the spray coating process to form LESS coating on different substrates. These substrates included ceramic, titanium, and carbon steel. Before the coating process, these substrates were all cleaned by isopropanol, ethanol, and deionized water. We first sprayed ~2 mL of silane solution onto the glass surface, and let the surface dry for 3 min. Then silicone oil (with a viscosity of 20 cSt) was sprayed onto the surface. The formation of the LESS coating was confirmed by the successful repellency of the dyed water (in blue).

Supplementary Video 4 shows a comparison between an uncoated and a LESS-coated ceramic substrates. Approximately 5 grams of synthetic feces (solid percentage 30%) was dropped onto the testing surfaces, and then rinsed by dyed water. The synthetic feces stick on the uncoated surface but slide off from the LESS-coated surface.

Supplementary Video 5 shows the water repellency comparison between a commercially available hydrophobic glaze coated toilet bowl (SloanTec®) and a LESS-coated toilet bowl. The blue liquid was dyed water.

Supplementary Video 6 shows the synthetic feces repellency comparison between a commercially available hydrophobic glaze coated toilet bowl (SloanTec®) and a LESS-coated toilet bowl. Approximately 5 grams of synthetic feces (solid percentage 30%) was dropped onto the testing surfaces from a height of ~10 cm.

Supplementary Video 7 shows a comparison between a LESS-coated surface and other control surfaces, including ceramic (a commonly used toilet material), Teflon, and silicone. Approximately 10 grams of human feces were dropped from a 75 mm height and landed on the testing surfaces. The feces stick on all three control surfaces except for the LESS-coated glass where the feces slide off from the surface.

Supplementary Video 8 shows the displacement wetting behavior of silicone oil on PDMS-grafted glass. We put a number of dyed deionized water droplets which were pinned onto the surface. Once the silicone oil was sprayed onto the surface, all water droplets started to slide off the surface due to displacement wetting of the silicone oil (i.e., the silicone oil displaces the water, and adheres onto the PDMS-grafted glass surface). The lubricated surface can then repel the immiscible dyed water demonstrating the stability of the lubricating layer.

Supplementary Note 1. Glass roughening and measurement of surface roughness

The glass surface (VWR) was intrinsically smooth with a roughness less than 1 nm. We created nanoscale porosity into the glass surfaces using an established protocol[1] by immersing them into 0.5 mol/mL sodium bicarbonate solution, and boiling for 48 hr. The micro-roughened glass was etched by two steps: first by using a universal laser systems VLS2.3 (35% power and 90% cutting speed) and then by buffered oxide etch (6:1 40% NH_4F in water to 49% HF in water) for 20 minutes at room temperature. The surface roughnesses of all these glass slides and other materials (e.g., ceramic, carbon steel, titanium, etc.) were measured either by an atomic force microscope (AFM) in peak-force-tapping mode or an optical profilometer from Zygo, shown in **Supplementary Table 4**.

Supplementary Note 2. Work of adhesion estimation

The work of adhesion, w_a, at the feces and substrate interface can be simplified as $w_a = 2(\gamma_{13} \cdot \gamma_{23})^{1/2}$ by the Girifalco and Good equation[2]. Healthy human feces contain ~70% of water[3] with the rest consisting of organic matters, some of which may lower the interfacial energy of the water-air interface. Therefore, we can estimate the upper bound of the surface energy (γ_{13}) of the feces to be similar to that of water[4] (i.e., $\gamma_{13} \leq$~72 mJ/m^2). From previous literature, glass surface[4] (γ_{23}) has surface energy as 310 mJ/m^2. Based on the Girifalco and Good equation, the work of adhesion between human feces and an untreated glass surface (w_{a0}) is $\leq$ 299 mJ/m^2.

There are three different methods to reduce the work of adhesion (**Supplementary Figure 1**). In the first method, a lubricating layer (silicone oil) can be added in between the feces and an untreated glass surface to reduce the adhesion. Since silicone oil is preferably to be absorbed to feces, only the surface energy of feces (γ_{13}) changes. Note that the silicone oil could be partially

or fully infused into the feces, therefore we assume that the surface energy of feces (γ_{13}) to be ~72 mJ/m^2 $\geqslant \gamma_{13} \geqslant$ ~21 mJ/m^2. As a result, the work of adhesion between the synthetic feces and a silicone-oil lubricated glass (w_{a1}) would be ~299 mJ/m^2 $\geqslant w_{a1} \geqslant$ ~161 mJ/m^2, leading to a maximum adhesion reduction of ~46% as compared to an untreated glass surface. The second method involves silanization of the glass surface with grafted-polydimethylsiloxane (PDMS). Since the grafted PDMS has nearly identical chemical structure as the silicone oil, one can assume their surface energies to be similar. The surface energy of silicone oil is measured to be ~21 mJ/m^2. Therefore, the work of adhesion between the synthetic feces and a PDMS-grafted glass (w_{a2}) would be ~78 mJ/m^2, resulting in a maximum adhesion reduction of ~74% as compared to an untreated glass surface. The third method involves coating a lubricating layer between the feces and a chemically treated glass so as to retain a thermodynamically stable lubricant layer on the substrate. In this case, we have ~72 mJ/m^2 $\geqslant \gamma_{13} \geqslant$ ~21 mJ/m^2, and $\gamma_{23} \approx$ 21 mJ/m^2. Therefore, the work of adhesion on the LESS-treated glass (w_{a3}) is ~78 mJ/m^2 $\geqslant w_{a3}$ $\geqslant$ 42 mJ/m^2, leading to a maximum adhesion reduction of ~86% as compared to an untreated glass surface. Overall, we have $w_{a1} > w_{a2} \geqslant w_{a3}$ and this trend is consistent with the experimental measurements.

Supplementary Note 3. Working conditions to form a stable lubricant layer

The formation of stable lubricant layer on a solid surface requires that 1) the lubricant should completely wet the solid surface and 2) cannot be displaced by immiscible foreign liquids. To achieve these conditions, the spreading parameter S and the disjoining pressure $\Pi(e)$ of the lubricant on the solid surface should be positive under air and foreign immiscible liquids of interest. Specifically, the spreading parameters under air (S_{ls}) and immiscible liquid (S_{lsf})

conditions can be calculated using a method proposed by van Oss, Chaudhury, and Good (vOCG) introduced in a recent publication[5], which are shown below:

$$S_{ls} = \sigma_s - (\sigma_{ls} + \sigma_l) = 2\sqrt{\sigma_s^{LW}\sigma_l^{LW}} + 2\sqrt{\sigma_l^+\sigma_s^-} + 2\sqrt{\sigma_s^+\sigma_l^-} - 2\sigma_l^{LW} - 4\sqrt{\sigma_l^+\sigma_l^-} \quad \text{(S1)}$$

$$\begin{aligned} S_{lsf} &= \sigma_{fs} - (\sigma_{ls} + \sigma_{fl}) \\ &= 2\sqrt{\sigma_s^{LW}\sigma_l^{LW}} + 2\sqrt{\sigma_f^{LW}\sigma_l^{LW}} + 2\sqrt{\sigma_l^+\sigma_s^-} + 2\sqrt{\sigma_s^+\sigma_l^-} + 2\sqrt{\sigma_l^+\sigma_f^-} + 2\sqrt{\sigma_f^+\sigma_l^-} \\ &-2\sqrt{\sigma_f^{LW}\sigma_s^{LW}} - 2\sqrt{\sigma_s^+\sigma_f^-} - 2\sqrt{\sigma_f^+\sigma_s^-} - 4\sqrt{\sigma_l^+\sigma_l^-} - 2\sigma_l^{LW} \end{aligned} \quad \text{(S2)}$$

Note that σ^{LW} indicates the Lifshitz-van der Waals component of the interfacial tension at an interface; whereas σ^+ and σ^- represent the acid and base terms of the polar component of the interfacial tension, respectively[5]. The solid surface here is grafted-PDMS-coated glass. The lubricant is silicone oil, and the foreign liquid is water. Interfacial tensions of different material interfaces of consideration are listed in **Supplementary Table 1**. The sign of disjoining pressure can be determined by Hamaker constant, which can be calculated with the dielectric constants and refractive indices of the materials of interest (see **Supplementary Table 2**). Based on the calculations from the spreading parameters and the disjoining pressures, silicone oil can spread completely onto PDMS-grafted smooth surfaces, and repel immiscible liquids, such as water. These predictions are consistent with our experimental observations.

Supplementary Note 4. Thickness characterization of PDMS-grafted layer

The XPS analyses were performed using a Kratos Analytical Axis Ultra instrument with monochromatic Al X-ray source ($h\nu$ = 1486.7 eV) operated at 280 W and a pressure of 10^{-9} torr. All samples were mounted under brass plates to minimize charging effects. A low energy electron flood gun was used for charge neutralization. The slight charging that occurred during the analysis was corrected by shifting the CH_x component of the carbon 1s spectra to 284.8 eV. Quantification was performed by applying relative sensitivity factors that account for differences

in escape depth as well as X-ray cross section. The takeoff angle between the sample surface plane and the electron analyzer was 90°.

The atomic percentage of silicon bond in PDMS was 7.3%, thus the approximate fraction of the XPS signal was 29% (7.3%×4). This accounts for the 1 O and 2 C atoms present in the PDMS. (Note that hydrogen cannot be detected by XPS and is thus excluded from this estimation). The inelastic mean free path (IMFP) of the Si 2p photoelectrons through a bulk PDMS is estimated to be 3.9 nm using an approach developed by M. Seah et al.[6]. The PDMS overlayer thickness was estimated by assuming a uniform overlayer model with IMFP of 3.9 nm and takeoff angle of 90°. Then the thickness of the grafted-PDMS layer on glass is 1.3 nm comprising ~29% of the signal.

Supplementary Note 5. Liquid repellency of LESS

We have evaluated the liquid repellency of our LESS coating using rainwater (pH = 5), surfactant solution or soapy water (at a critical micelle concentration of 8 mM of sodium dodecyl sulfate, SDS), synthetic hard water (i.e., 250 mg/L of calcium carbonate in water), and alkaline solution (pH meter calibration solution, pH = 10). The surface tension of above liquids was measured through pendent drop method and is summarized in **Supplementary Table 6**. We note that the soapy water was used to emulate contaminated water with organic contaminants. We used the synthetic hard water to demonstrate that LESS can potentially prevent or reduce mineral build-up in current toilets by repelling hard water droplets. Note that over 80% of the United States has hard water, which is typically defined as water with calcium carbonate concentration over 60 mg/L (https://water.usgs.gov/owq/hardness-alkalinity.html). The hard water issue poses a major issue in toilet cleaning due to buildup of minerals that are difficult to remove. Moreover, mineral buildup makes toilet surfaces more prone to residue and bacteria fouling.

To evaluate the liquid repellent performance of LESS (lubricant thickness < 1 μm) against different liquids, we have measured the contact angle and contact angle hysteresis of each test liquids, which are summarized in **Supplementary Figure 3** and **Supplementary Table 7**. We have further evaluated the durability of LESS under the impact of 10000 liquid drops. To conduct these tests, 10 μL of droplet was continuously released on LESS-coated glass at a height of 10 mm, and the surface was tilted with 45°. After the drop dripping test, the contact angle and contact angle hysteresis were measured, as shown in **Supplementary Figure 3** and **Supplementary Table 8**. We noticed that contact angle hysteresis increased after the drop dripping test as the lubricant was depleted by the impact and shear forces from the drop impact. We note that for a surface with strong liquid repellency, the contact angle hysteresis typically would not be higher than ~15% of the static contact angle[7]. The contact angle hysteresis of different liquids on the LESS-coated surface are generally within 10% of the static contact angles of the corresponding test liquids (except for alkaline water, whose contact angle hysteresis is ~20% of its contact angle after 10000 dripping drops). Therefore, the LESS-coated samples are still considered to be highly repellent to rainwater, soapy water, and hard water even after 10000-droplet dripping.

Furthermore, we have verified that our measured contact angles on LESS-coated glass are consistent with the predictions by a recent theoretical model for apparent contact angles of liquid droplets on lubricated surfaces[8-10]. The apparent contact angle of water on LESS with silicone oil (20 cSt) can be predicted by the following Equation S3:

$$\cos\theta_{app} = \frac{\gamma_{OV} - \gamma_{OW}}{\gamma_{WO} + \gamma_{OV}} \tag{S3}$$

where θ_{app} is the apparent contact angle, γ_{OV} and γ_{OW} are interfacial tension of oil-vapor and oil-water, respectively. We have measured the interfacial tension through the pendent drop method

and the results are summarized in **Supplementary Table 5**. Based on Equation S3 [10], we have calculated the apparent contact angle of water on LESS-coated glass to be 102.1°, which is in close agreement to our measured value (103.8±0.1°) as shown in **Supplementary Table 7**.

Supplementary Note 6. Simulated toilet flushing

To simulate the condition of toilet flushing, we designed an open channel flow system with 50 mm width, in which the flow rate can be precisely controlled. After measuring the height of the flowing water level where the sample (i.e., synthetic feces) is located, we calculate the hydraulic diameter as:

$$D_h = 4R_h = \frac{4A}{P} \tag{S4}$$

where A is the flow area cross section, and P is the wetted perimeter. Based on the hydraulic diameter, we can then estimate the Reynolds number as:

$$\mathrm{Re}_D = \frac{\rho v D_h}{\mu} \tag{S5}$$

where v is the flow velocity, ρ is the water density, μ is the dynamic viscosity. Since all the open-channel flow under investigations have Reynolds numbers ≥2500, these flows are in turbulent flows and the wall shear can be estimated as:

$$\tau_w = \frac{0.0225(\mu(a+2h))^{0.2}\rho^{0.8}\dot{V}^{1.8}}{4a^2h^2} \tag{S6}$$

where a is the flow width, h is the flow height, and V is the volume flow rate[11]. We also measured the height of the flowing water level in a real toilet where the tilting of the surface is ~45°, and performed the same open channel flow calculation. A typical dual flush toilet consumes either 0.8 or 1.6 gallon per flush (gpf), and each flush take approximately 5 s. The

flow parameters and toilet geometries were estimated as follow: 600 mm flow width, 300 mm from flushing outlet, and 3.97 mm flow height for 1.6 gpf, and 3.50 mm flow height for 0.8 gpf. Based on these parameters, the Reynolds number is estimated to be ~177000 and the corresponding wall shear values range from 0.11 Pa to 0.78 Pa. The wall shear in our open channel system under different flow rate is calculated as shown in **Supplementary Table 11**. Note that the wall shear in our system is in the same order of magnitude as those calculated for the real toilet. Therefore, the open channel flushing system can realistically simulate the real toilet flushing condition.

Supplementary Note 7. Rainwater bacteria identification

50 µL of rainwater was spread uniformly onto four different agar mediums: Thermo Scientific™ Blood Agar (TSA with Sheep Blood) Medium, Thermo Scientific™ MacConkey Agar Medium, BD BBL CHROMagar Orientation, and BD BBL MHB agar. Then the bacteria were incubated for 24 hours. Isolates were prepared for analysis using a direct transfer method following a standard Bruker protocol. Individual colonies from 24-hour cultures were transferred onto a MALDI target plate using a sterile pipette tip and allowed to dry. The cells were lysed by applying 1 µL of 80% formic acid solution in water, samples were allowed to dry and 1 µL of 10 mg/mL HCCA matrix solution in 50% aqueous acetonitrile containing 2.5% trifluoroacetic acid was applied to each sample and allowed to dry. A bacterial test standard (BTS; Bruker Daltonics) was used for instrument calibration and as a positive control. Matrix blank spots were included in each analysis to ensure that the target plate was thoroughly cleaned and there is no carryover signal. MALDI mass spectra were acquired on a Bruker Ultraflextreme MALDI TOF/TOF mass spectrometer in the linear, positive-ion mode. Spectra were processed using a factory default processing method for the Biotyper application and searched against a Bruker library containing

entries of 6903 cellular organisms using MALDI Biotyper Version 3.1 software (Bruker). The results are shown in **Supplementary Table 12**.

Supplementary Note 8. Bacteria fouling test using feces

We have conducted the anti-bacterial experiment using synthetic feces spiked with *Escherichia coli* (*E. coli.*) with a concentration of 10^8 cfu/ml. Note that *E. coli* is a common bacteria found in human feces[12] and the concentration of an individual species in stool sample can range from 10^4 – 10^8 cfu/ml[13]. Before conducting the bacteria fouling experiment, we first confirmed that *E. coli* was successfully spiked into the synthetic feces. To confirm this, synthetic feces with 30% solid content was prepared by incorporating *E. coli* solution (10^8 cfu/ml). The *E. coli.* spiked feces were then placed in contact with a control surface (e.g., glass slides) and rinsed with water to remove any solid residues. The glass slides were covered with solid agar after rinsing and incubated at 37 ^{o}C for 24 hours. The numbers of bacteria colonies were then counted to quantify the level of bacterial contamination on the control surfaces. We performed the same experiment on glass slide without spiking *E. coli*, and the comparison is shown in **Supplementary Figure 12**. The surface in contact with *E. coli* spiked feces had at least 5 times more bacteria colonies than the surface in contact with regular synthetic feces.

For the bacterial fouling test on LESS and control surfaces, synthetic fecal wastes with 10%, 30%, and 50% solid content were prepared. We used *E. coli* with a concentration of 10^8 cfu/ml in water to spike the bacteria into the synthetic feces. Then ~20 gram of synthetic feces was in full contact with LESS coated and uncoated glass for 1 min. Then the surfaces were cleaned by rinsing with sterilized water to simulate the flushing after the feces contact. We then incubated the surface with solid agar for 24 hours and count the number of *E. coli* colony. No visible

bacteria colonies were found on LESS-coated glass; however, the untreated glass surfaces were contaminated with a number of bacteria colonies (**Supplementary Figure 13**).

Supplementary Note 9. Working conditions for displacement wetting

A critical criterion for displacement wetting is that the solid must be preferably wetted by the lubricant rather than by the foreign liquid one wants to repel. To determine whether a solid will be wetted by liquid B (lubricant) when liquid A (foreign liquid) already adheres onto the surface, we compare the total interfacial energy of the individual wetting configurations. Specifically, configuration A refers to the state where the smooth solid is wetted by the foreign liquid, and configuration B refers to the state where the smooth solid is wetted by the lubricant. E_A and E_B represent the total interfacial energies per unit area of the wetting configuration A and B, respectively. And σ_{sf}, σ_{sl}, σ_f, and σ_l represent the interfacial tensions of the solid-immiscible fluid interface, solid-lubricant interface, immiscible fluid-vapor interface, and lubricant-vapor interface, respectively. In order for the lubricant to displace the foreign liquid and preferentially attach onto the solid substrate, wetting configuration B should be at a lower energy state. To derive a thermodynamic relationship for the displacement wetting from configuration A to configuration B, we have $E_A - E_B > 0$, which can be further expressed as,

$$\Delta E = \sigma_{sf} - \sigma_{sl} > 0 \tag{S7}$$

In particular, (S7) is reduced to experimentally measurable quantities with the use of the Young equation[4], where we have,

$$\Delta E = \sigma_l \cos\theta_l - \sigma_f \cos\theta_f + \sigma_f - \sigma_l > 0 \tag{S8}$$

where θ_l and θ_f, are the equilibrium contact angles of the lubricant and the foreign immiscible liquid on a flat solid surface, respectively. Our experimental measurements (i.e., σ_f = 71.1±0.2 mN/m (water), σ_l = 20.7±0.3 mN/m (silicone oil), θ_f = 106.5°±0.4°, θ_l = ~ 0°) have shown that

Eq. (S8) is satisfied (i.e., ΔE = 91.3 mN/m > 0) for the displacement wetting of the lubricant on our experimental system.

Supplementary Note 10. Minimal flush water test on toilets

To estimate the minimal water needed for flushing the bulk waste from a single defecation through the drain line and toilet trapway in the current toilet system, we used a modified maximum performance (MaP) flushing test protocol (https://www.map-testing.com/map-testing-protocol.html). Specifically, 130 g of synthetic feces with 30% solid content were used to simulate the bulk fecal waste. The reason we used this amount of feces is that humans on average eliminate 128 g of fresh feces per person per day[14]. In addition, the synthetic feces with 30% solid content have similar rheology properties compared to healthy human fecal waste[15,16]. In the test, we gradually reduced the water volume in the tank to flush the synthetic feces until the feces can no longer be completely flushed down the toilet. In a commercial 1.6 gpf (i.e., 6 Lpf) toilet, ~2.2±0.1 liters is sufficient to flush down the synthetic fecal waste (i.e., 130 gram), shown in **Supplementary Figure 17**. As a LESS-coated surface only needs ~10% of the flushing water to clean the surface, the water saving in current flush toilet system by adopting the LESS coating is estimated to be up to ~63±2%.

Supplementary Note 11. Analysis of environmental impact

Silicone oil is approved by the Food and Drug Administration (FDA) for eye care[17] and surgical applications[18] and has been widely used in cosmetic industry[19]. As an estimation, if all silicone oil content in the make-up is washed away from our skin and drained into the environment directly, it is estimated that at least ~1.3×10^8 kg silicone oil will be released to the environment every year based on the silicone oil market value and price[20].

From our experimental estimation, it is determined that 60 minutes of water flushing at 2.5 gpm flow is required in order to completely deplete an 8 μm-thick silicone oil layer on a 75×25 mm^2 glass slide (Fig. 6a in the main text). Therefore, we have estimated that the leakage of the silicone oil into the water would be on the order of ~0.03 ppm. In addition, it is estimated that over 141 billion liters of water is consumed globally everyday by toilet flushing alone. Assuming every existing toilet in the world is coated with our LESS coating as an upper limit estimate, the total silicone oil flushed down the toilets is estimated to be ~1.2×10^6 kg/year, which is <1% of the current silicone oil leaking from the cosmetics industry alone.

Supplementary Figures

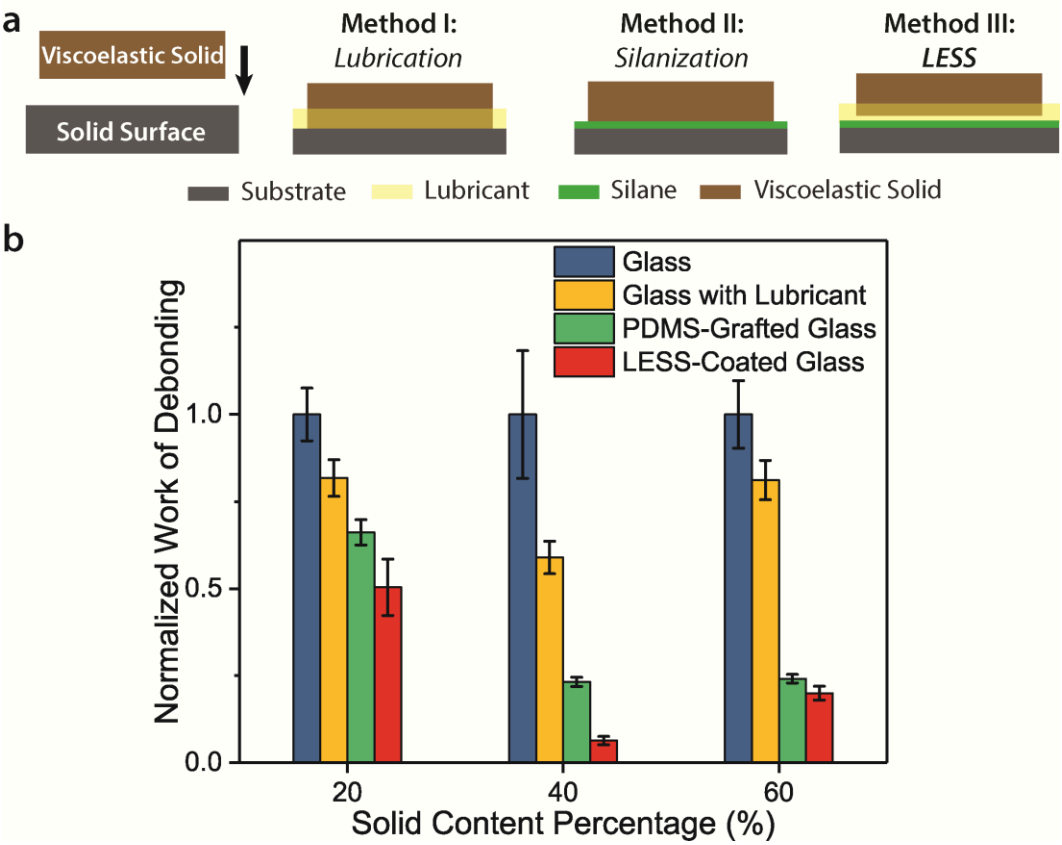

Supplementary Figure 1. Schematics showing three methods to reduce the work of adhesion and the corresponding experimental adhesion measurement results. a, Adhesion of viscoelastic solids (left to right) on an untreated surface; a lubricated surface without chemical treatment; a silanized surface; and a lubricated surface with silanization treatment. **b,** Measurements of adhesion between synthetic feces and various surfaces. The work of debonding of each surface is normalized by that of bare glass for the respective solid content. All error bars represent standard deviations of at least four independent measurements.

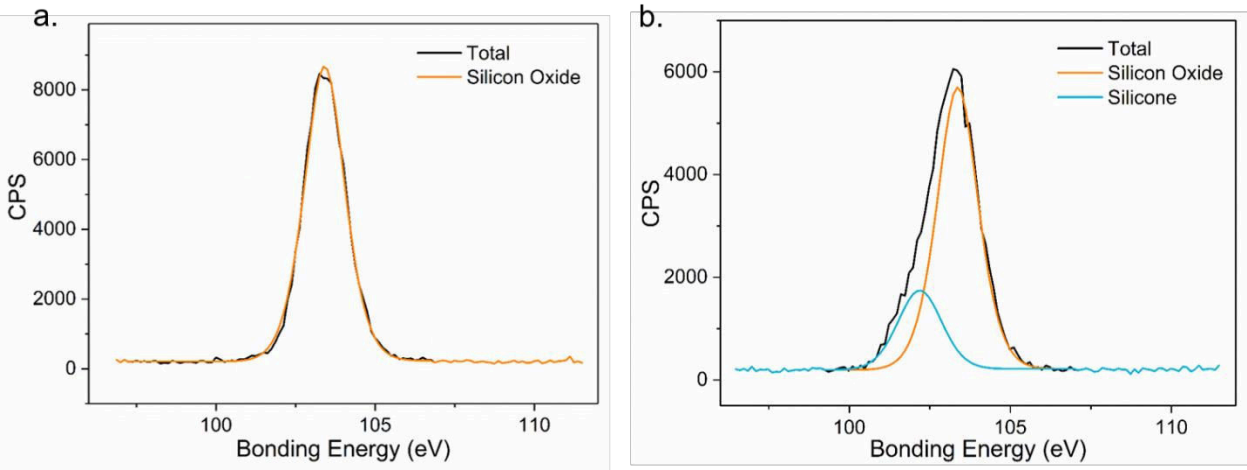

Supplementary Figure 2. XPS characterizations of silicon element on untreated (e.g. glass) and PDMS-grafted substrates. a, The peak of silicon element is originated from silicon dioxide, which is the main component of glass. **b,** The peak of silicon element (Si 2p) is originated from silicon dioxide and silicone, which confirmed the presence of the PDMS on the PDMS-grafted substrate. CPS is an abbreviation for count per second.

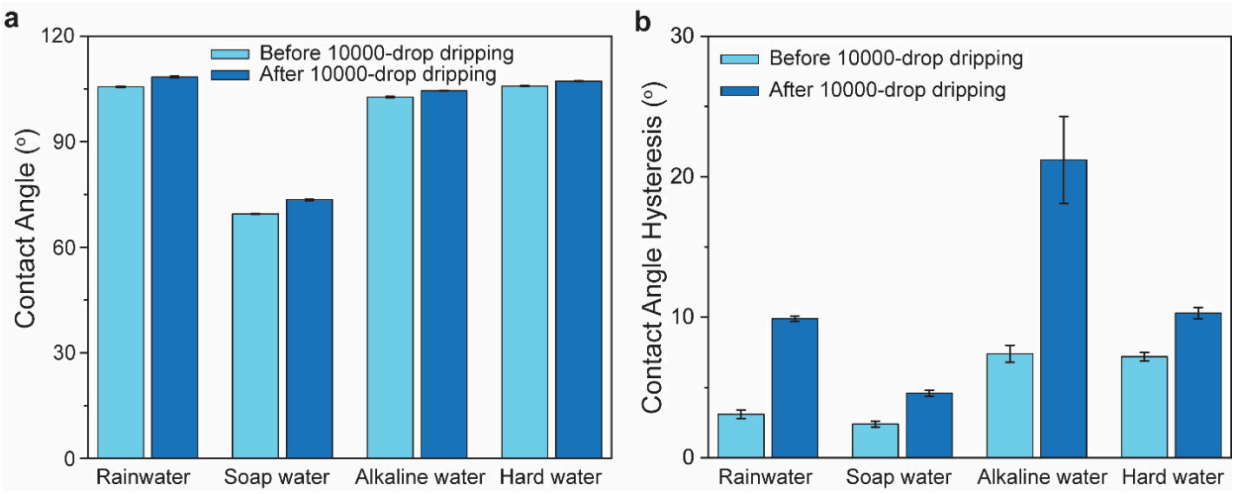

Supplementary Figure 3. Plots showing (a) contact angle and (b) contact angle hysteresis of various liquids on LESS-coated surfaces before and after 10000-droplet dripping. All error bars represent standard deviations of three independent measurements.

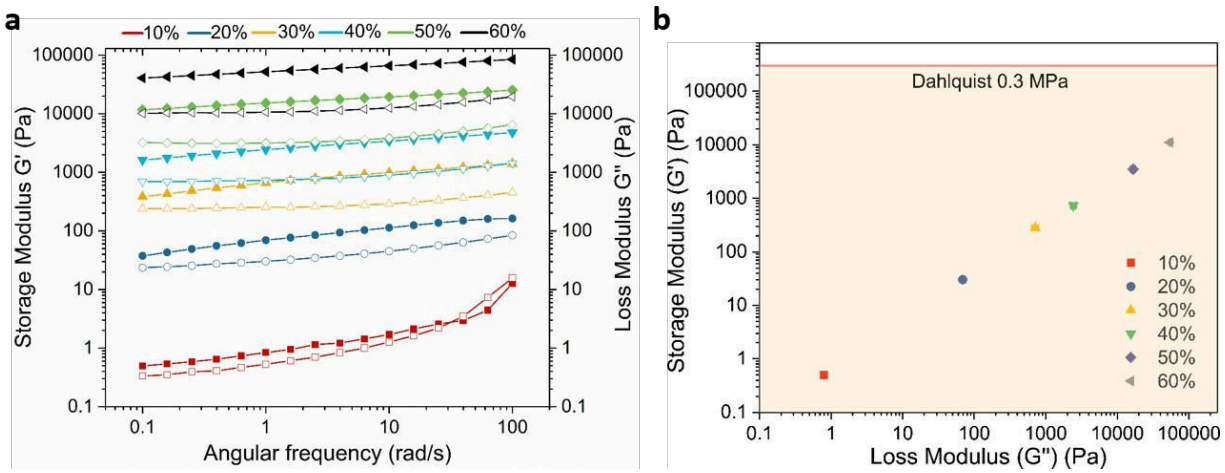

Supplementary Figure 4. Viscoelasticity of synthetic feces. a, The storage and loss moduli of synthetic feces with different solid content fraction (e.g. 10%, 20%, 30%, 40%, 50%, and 60% of solids in synthetic feces). The solid and open symbols represent the storage modulus and the loss modulus, respectively. **b,** Comparison of the Dahlquist criterion with the measured storage moduli of different synthetic feces. The storage moduli of synthetic feces with different solid content fraction (e.g. 10%, 20%, 30%, 40%, 50%, and 60% of solid contents in synthetic feces) under frequency of 1 rad/s. The error bars represent standard deviations of storage moduli from three independent measurements.

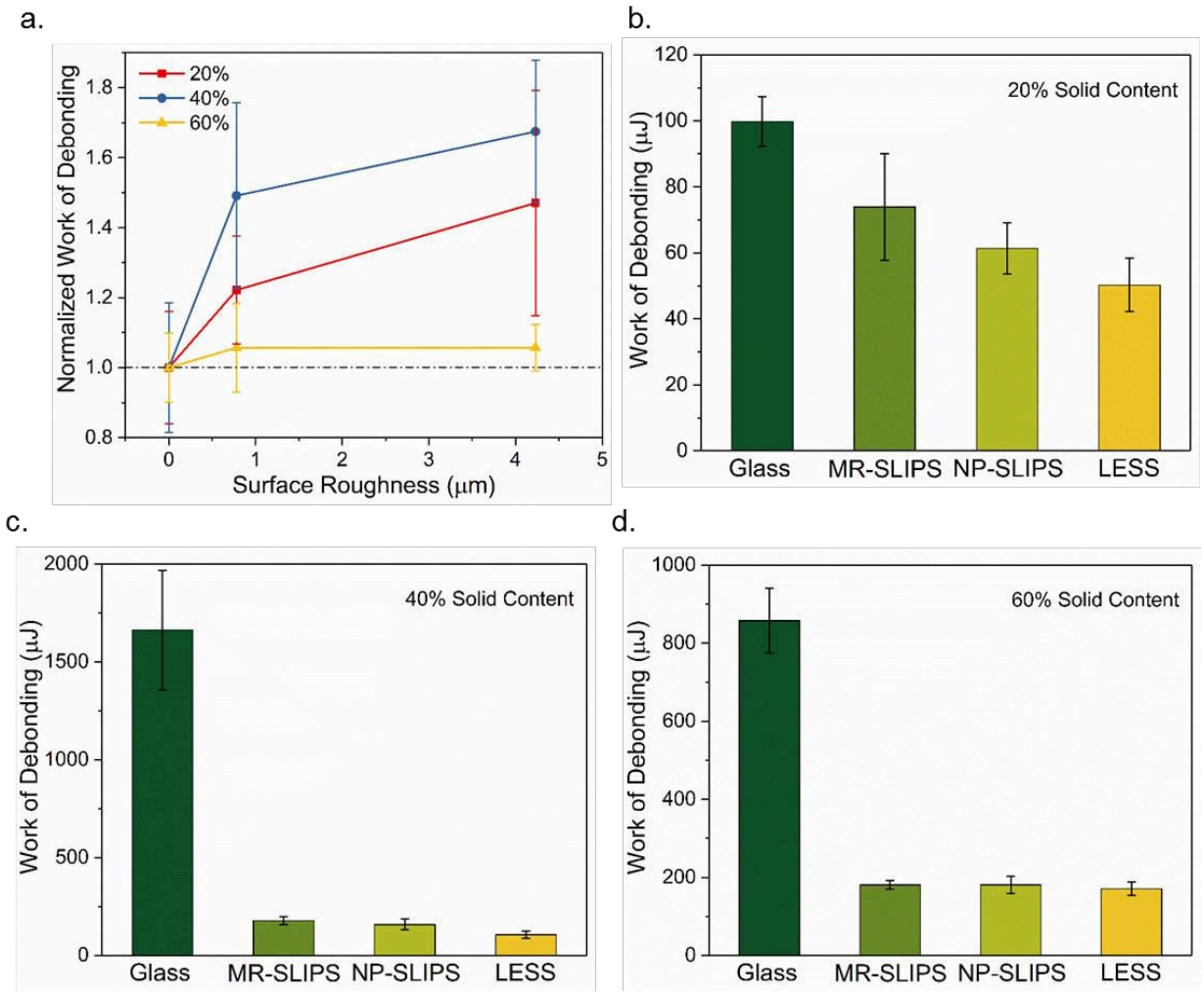

Supplementary Figure 5. Adhesion measurement of four different surfaces: glass, micro-roughened slippery liquid-infused porous surfaces (MR-SLIPS), nano-porous slippery liquid-infused porous surfaces (NP-SLIPS), liquid-entrenched smooth surfaces (LESS). a, Work of debonding of synthetic feces of varying solid contents of surfaces with different roughness. The data is normalized by the work of debonding of 40% solid content synthetic feces on LESS. **b, c, d,** Work of debonding was measured with synthetic feces of different solid content percentage (20%, 40%, and 60%). Standard deviations of the work of debonding were obtained from at least 5 independent measurements. The lubricant used for SLIPS and LESS was silicone oil with a viscosity of 20 cSt. All error bars represent standard deviations of four to six independent measurements.

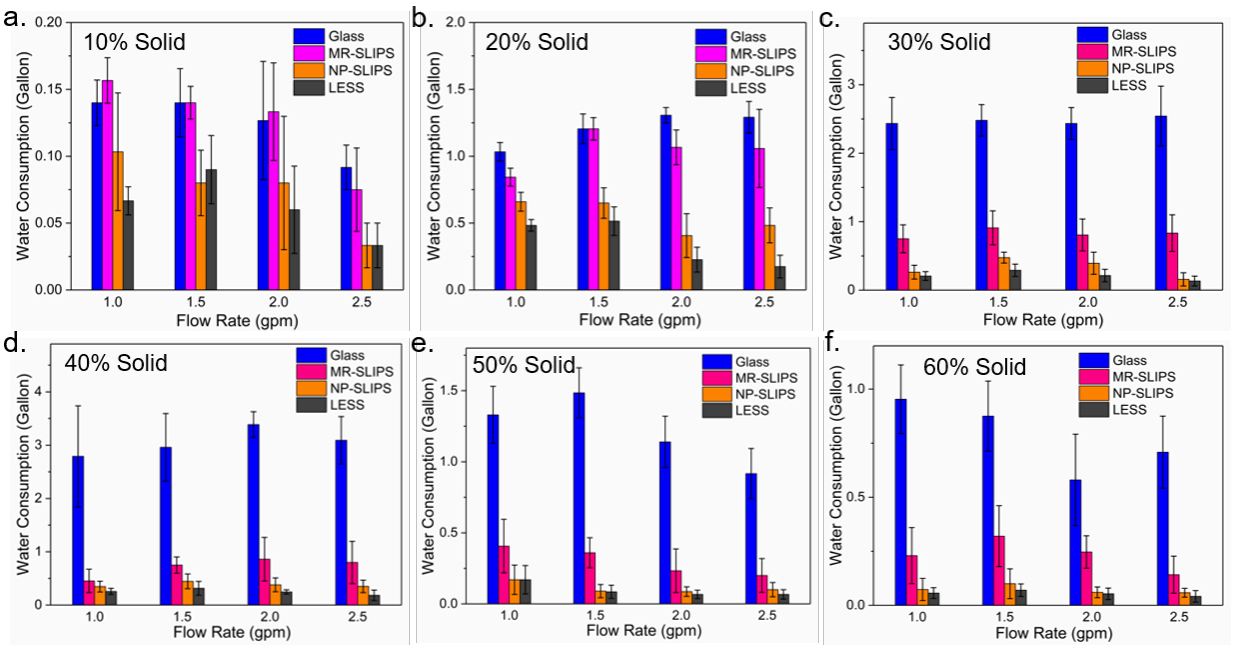

Supplementary Figure 6. Cleaning water consumption measurements on four different surfaces under different flow rates. a, b, c, d, e, f, Water consumption performances of four different surfaces (glass, MR-SLIPS, NR-SLIPS and LESS) after impact of synthetic feces with different solid content percentage (10%, 20%, 30%, 40%, 50%, and 60%). All error bars represent standard deviations of at least 4 independent measurements.

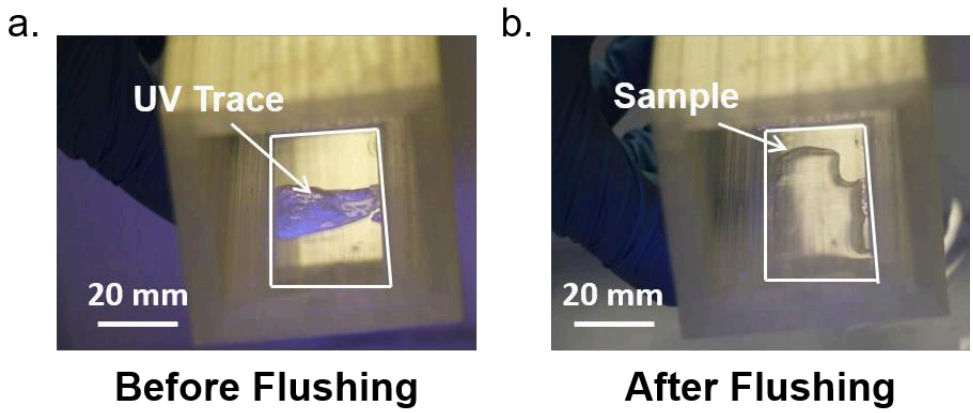

Supplementary Figure 7. Fluorescence tracing on feces contamination on the test samples (highlighted in white box). a, Fluorescent particles (0.3 wt%) were added to synthetic feces. The synthetic feces shown here had 20% solid content, and the test surface was untreated glass. **b,** A surface is considered clean once there was no observable fluorescence after flushing.

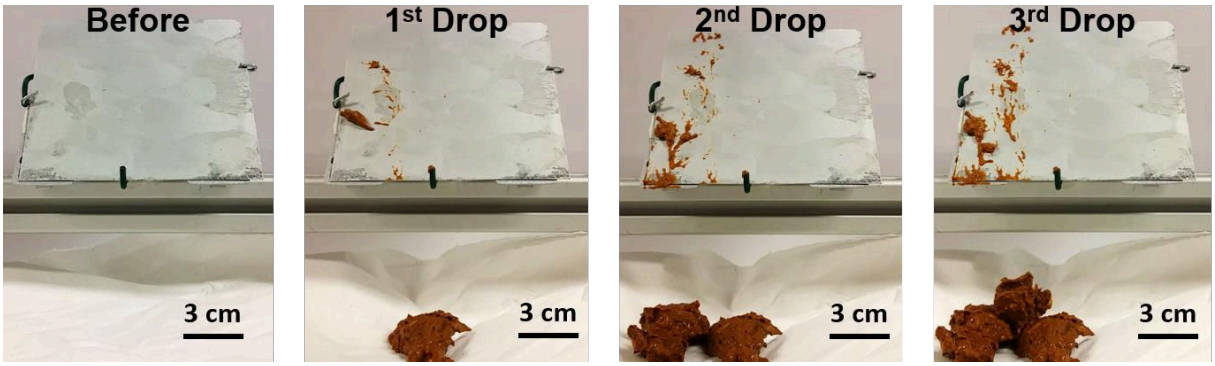

Supplementary Figure 8. Human feces dropping test on a SLIPS-coated aluminum. SLIPS-coated aluminum has an underlying surface roughness ~1 μm. The lubricant used here is DuPont™ Krytox 101 (viscosity ~18 cSt), whose viscosity is similar to the silicone oil (viscosity 20 cSt) used on LESS. The human feces (~10 grams) were dropped from ~80 mm height. After 1 –3 feces drops, the SLIPS-coated aluminum has left with feces residue.

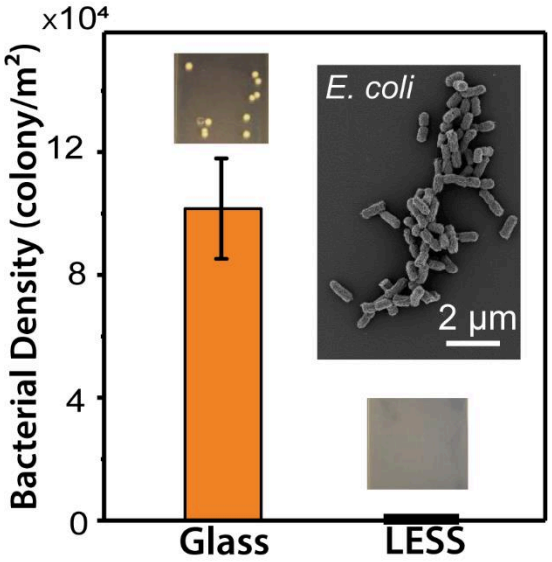

Supplementary Figure 9. Bacteria adhesion test with *Escherichia coli* spiked synthetic urine on different surfaces. The inset image shows an SEM image of *E. coli*. The dimensions of the inset optical image showing bacteria colonies are 10 mm × 10 mm. Error bars represent standard deviations of three independent measurements.

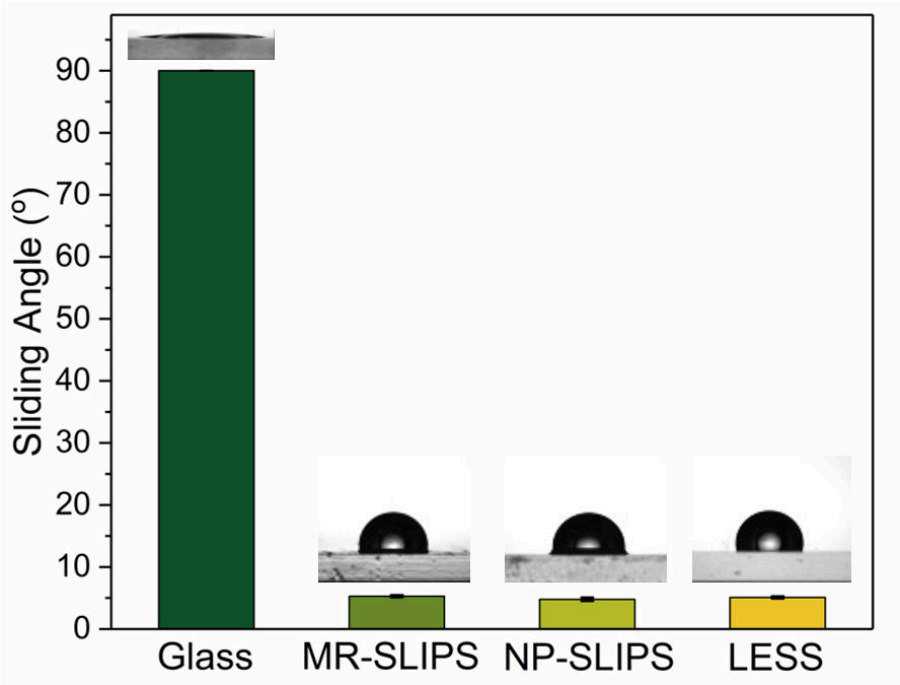

Supplementary Figure 10. Sliding angle measurement of 10 µL *E. coli* spiked synthetic urine on four different surfaces: glass, SLIPS with micro-roughened glass substrate (MR-SLIPS), SLIPS with nano-roughened glass substrate (NP-SLIPS), and LESS. All error bars represent standard deviations of four independent measurements by a goniometer.

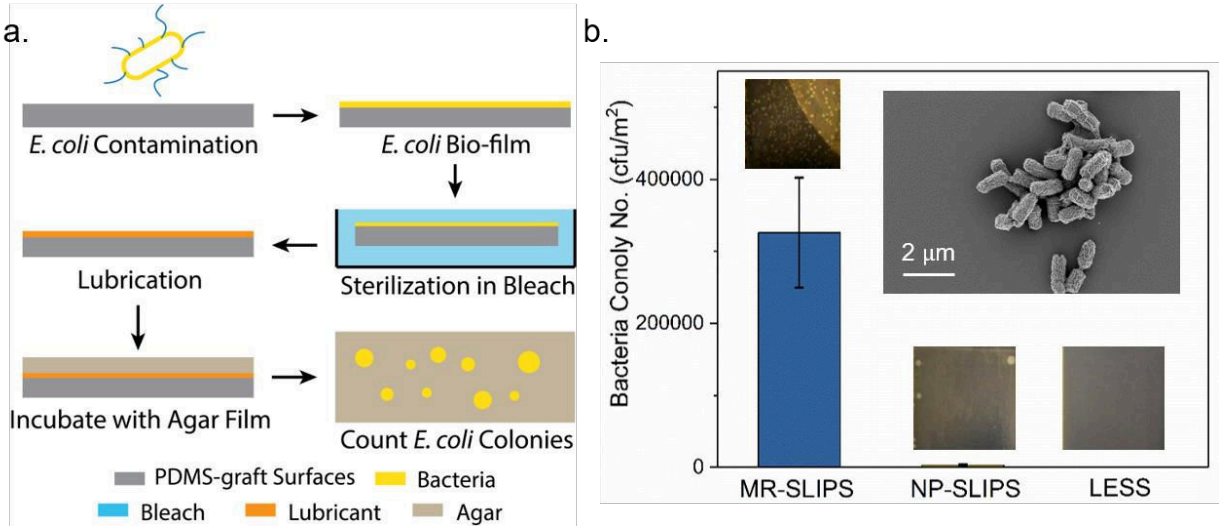

Supplementary Figure 11. Sterilization test on PDMS-grafted surfaces with different surface roughness. a, Experimental procedures for testing sterilization on these surfaces. All surfaces were contaminated with *E. coli* biofilm, and then sterilized with bleach and 70% of alcohol for 10 min before lubrication with sterilized silicone oil. Afterwards, all surfaces were lubricated and incubated with agar film for 36 hours. **b,** The bacterial colonies grow on surfaces with underlying roughness (SLIPS with micro-roughened glass substrate (MR-SLIPS)) while little or no bacteria are found on SLIPS with nano-roughened glass substrate (NP-SLIPS) and LESS-coated surfaces. The inset image shows a SEM image of *E. coli*. This suggests that if these surfaces were contaminated (e.g., during an application of interest, if lubricant was depleted), LESS-coated surfaces could be readily sterilized, and their anti-biofouling function could be restored. The dimensions of the inset optical image showing bacteria colonies are 10 mm × 10 mm. All error bars represent standard deviations of three independent measurements.

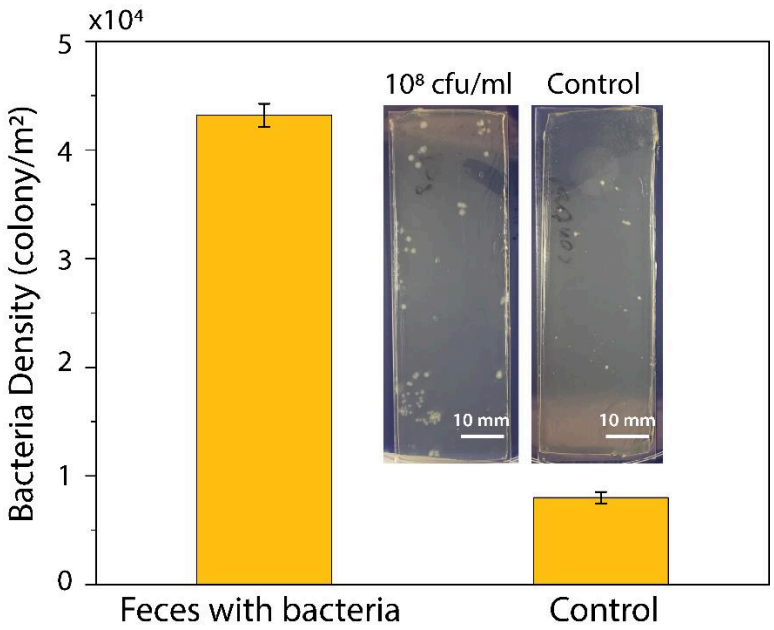

Supplementary Figure 12. Surface fouling with synthetic feces spiked with and without bacteria. Optical images showing the comparison between feces spiked with bacterial (10^8 cfu/ml) and without (control). Error bars represent standard deviations of three independent measurements based on colonies counting using ImageJ.

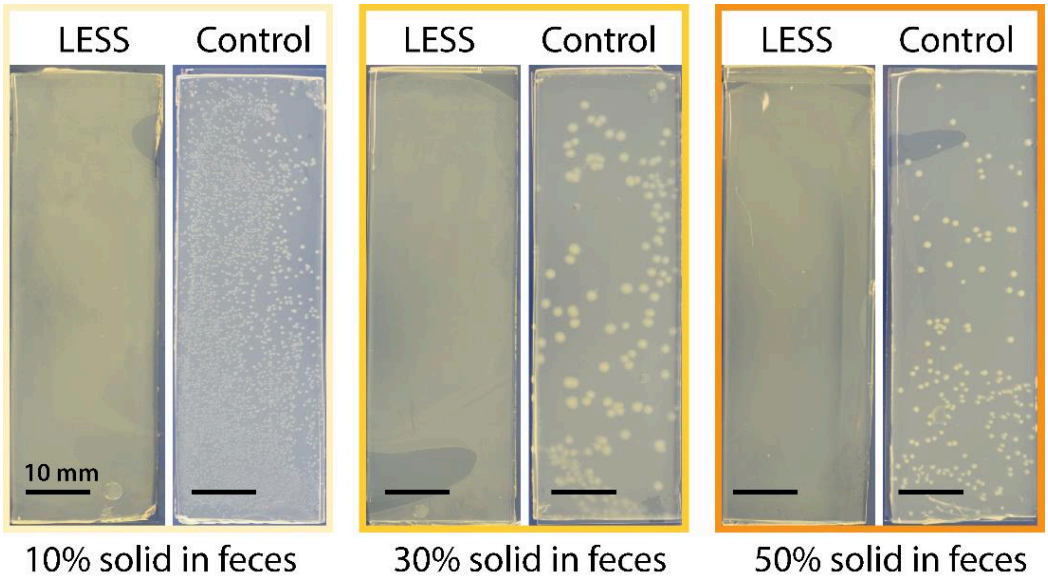

Supplementary Figure 13. Optical images showing the bacteria colonies on different surfaces after simulated defecation contamination with bacteria spiked synthetic feces at different solid content percentage (10%, 30%, and 50%). All scale bars are 10 mm.

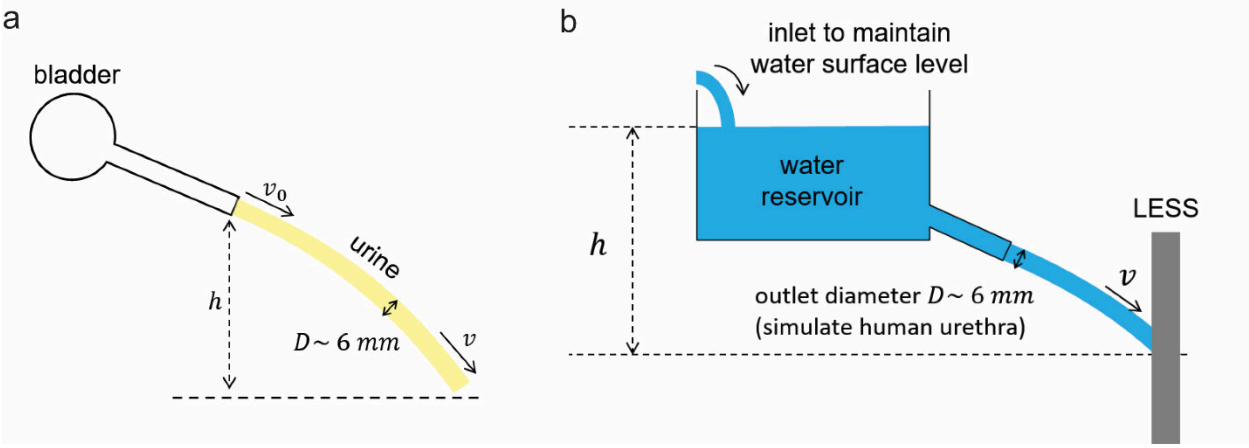

Supplementary Figure 14. Schematic showing (a) a physical model and (b) a flow setup to emulate the process of human urination.

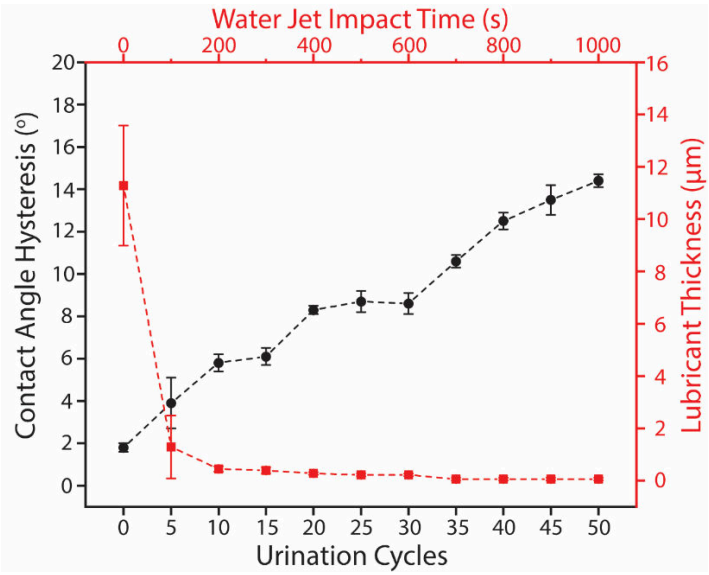

Supplementary Figure 15. Contact angle hysteresis of water and the lubricant thickness of the LESS coating against different urination cycles. Error bars represent standard deviations from at least three independent measurements.

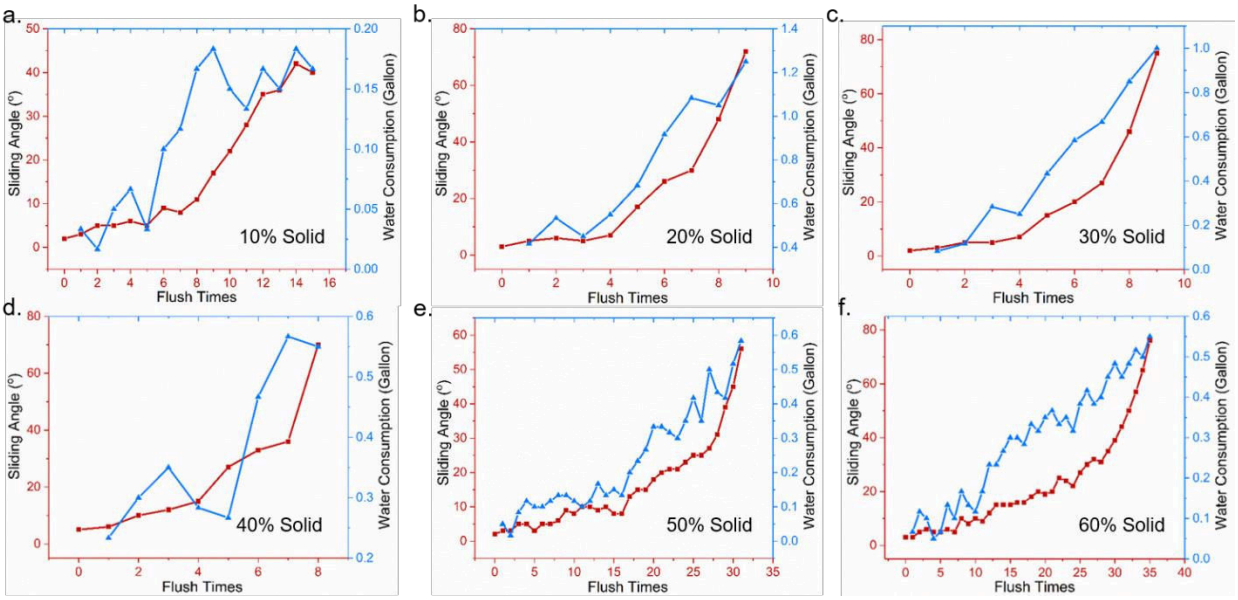

Supplementary Figure 16. Durability tests of LESS-coated glass under feces impact and water flushing cycles. a, b, c, d, e, f, Synthetic feces with different solid content percentage (10%, 20%, 30%, 40%, 50%, and 60%) were used in these tests. Each test was performed at least 3 times, and the charts shown here are one of the representative results. The red data points refer to the sliding angle, whereas the blue data points represent water consumption.

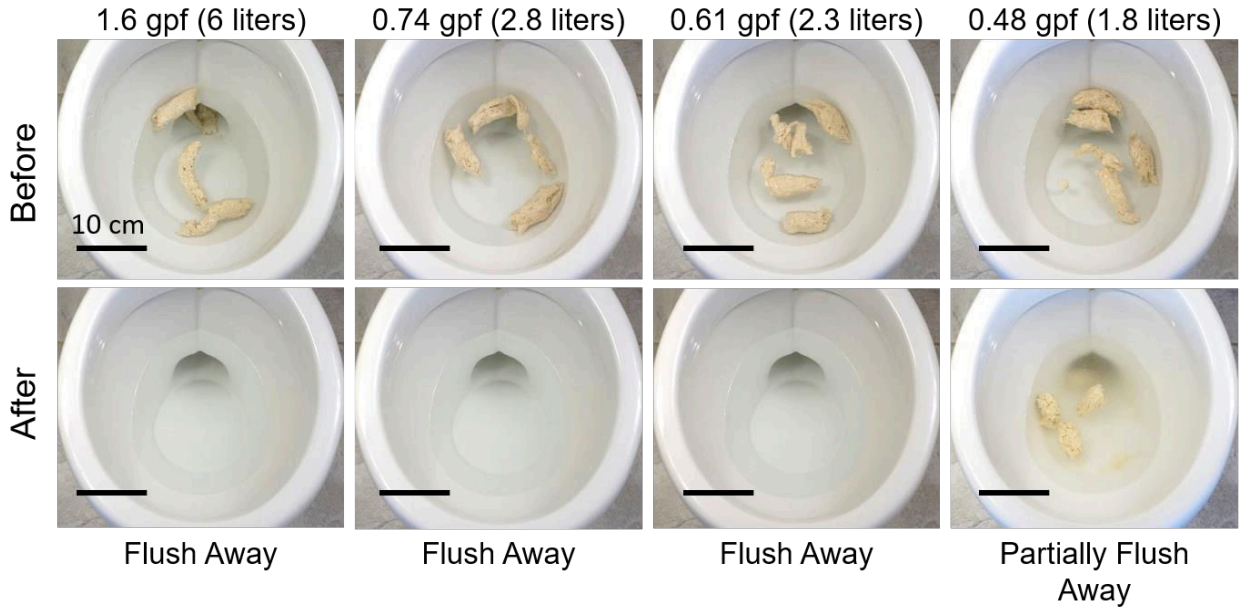

Supplementary Figure 17. Modified maximum performance (MaP) flushing test for minimal flush water measurement. About 2.2±0.1 liters of water would be required to flush down 130 grams of synthetic feces in a commercial toilet with 1.6 gpf (i.e., 6 liters per flush). Three independent measurements were performed. All scale bars are 10 cm.

Supplementary Tables

Supplementary Table 1. Surface energy components for materials at ambient environment.

Materials	**σ (mN/m)**	**σ^{LW} (mN/m)**	**σ^{+} (mN/m)**	**σ^{-} (mN/m)**
Grafted-PDMS	20.7	20.7	0	0
water	72.8	22.6	25.5	25.5
silicone oil	20.7	20.7	0	0

Note: The interfacial tension values of water in the table were obtained from reference[5]. Note that silicone oil is known to be non-polar[21]. The interfacial tension values of silicone oil were obtained from our experimental measurements. Note that distinct from the cross-linked bulk PDMS, our PDMS-grafted surfaces are non-cross-linked and display liquid-like behaviors. Therefore, the surface tension of silicone oil (with the same chemistry as PDMS) is used for the calculation.

Supplementary Table 2. Calculated spreading parameters (*S*) and Hamaker constant (*A*) for liquids on PDMS-grafted glass.

solid	**lubricant**	**foreign fluid**	ϵ_s	n_s	ϵ_l	n_l	ϵ_f	n_f	***A*** **(10^{-21}J)**	***S*** **(mN/m)**	**stable lubrication**
PDMS	silicone	air	2.32	1.4	2.6	1.41	1	1	2.07	0	Y
PDMS	silicone	water	2.32	1.4	2.6	1.41	80	1.33	0.233	0	Y
PDMS	water	silicone	2.32	1.4	2.6	1.41	2.1	1.3	0.564	−102.0	N
PDMS	water	air	2.32	1.4	80	1.33	1	1	−8.42	−102.4	N

Note: All dielectric constants and refractive indices listed in the table were obtained from reference[2] and [22].

Supplementary Table 3. Contact angle and contact angle hysteresis on the PDMS-grafted coating.

	Contact Angle (^{o})	Advancing/Receding Angle (^{o})	Contact Angle Hysteresis (^{o})
DI water	102.9±0.1	109.3±0.6/102.5±0.4	6.8±0.5

Note: All data was collected from 5 independent sessile-drop measurements. 10 μL drop was used for the contact angle measurement. Droplet addition and retraction method with a flow rate of 0.5 μL/s was used for the contact angle hysteresis measurement.

Supplementary Table 4. Surface roughness of various base substrates.

Materials	Ceramic	Carbon Steel	Titanium	Glass with micro-roughness	Glass with nano-roughness
R_a (nm)	598 ± 35	451 ± 50	661 ± 30	4120 ± 260	870 ± 60

Note: R_a is measured based on an area of 478 μm by 478 μm.

Supplementary Table 5. Interfacial tension of silicone oil-water, silicone oil-vapor and water-vapor.

	Silicone oil-Water	Silicone oil-Vapor	Water-Vapor
Interfacial Tension (mN/m)	31.7±0.1	20.7±0.3	72.8±0.4

Note: All data was collected from 3 independent pendent-drop measurements.

Supplementary Table 6. Surface tension of various liquids.

	DI water	Rainwater	Soapy Water	pH=10 solution	Hard water
Surface Tension (mN/m)	72.8±0.4	71.7±0.1	37.3±0.2	70.5±0.4	72.9±0.1

Note: All data was collected from 3 independent pendent-drop measurements.

Supplementary Table 7. Contact angle and contact angle hysteresis on LESS coatings.

	Contact Angle (^{o})	Advancing/Receding Angle (^{o})	Contact Angle Hysteresis (^{o})
DI water	103.8±0.1	104.6±0.2/103.1±0.1	1.5±0.1
Rainwater	102.0±0.2	104.4±0.5/101.3±0.2	3.1±0.3
Soapy Water	69.5±0.1	69.8±0.1/67.4±0.4	2.4±0.2
pH=10 solution	102.7±0.2	104.5±0.2/97.1±0.8	7.4±0.6
Hard water	105.8±0.1	106.5±0.2/99.3±0.5	7.2±0.3

Note: All data was collected from 5 independent sessile-drop measurements. 10 μL liquid drop was used for contact angle measurement. Droplet addition and retraction method with a flow rate of 0.5 μL/s was used for the contact angle hysteresis measurement. The lubricant thickness is ~<1 μm.

Supplementary Table 8. Contact angle and contact angle hysteresis on LESS coatings after 10000-drop impact.

	Contact Angle (^{o})	Advancing/Receding Angle (^{o})	Contact Angle Hysteresis (^{o})
Rainwater	108.4±0.2	110.3±0.4/100.4±0.2	9.9±0.2
Soapy water	73.5±0.2	76.1±0.2/71.5±0.3	4.6±0.2
pH=10 solution	104.5±0.1	111.6±0.4/90.4±3.2	21.2±3.1
Hard water	107.2±0.1	110.1±0.3/99.8±0.3	10.3±0.4

Note: All data was collected from 5 independent sessile-drop measurements. 10 μL liquid drop was used for contact angle measurement. Droplet addition and retraction method with a flow rate of 0.5 μL/s was used for the contact angle hysteresis measurement.

Supplementary Table 9. Compositions of the synthetic feces.

Ingredients	% dry mass	Nutrition
Yeast	32.49	Biomass
Psyllium	10.84	Fibre
Peanut oil	17.31	Fat
Miso	10.84	Fibre/Protein/Fat
Polyethylene glycol	12.14	Carbohydrate
Calcium phosphate	10.84	Biomass
Cellulose	5.53	Carbohydrate

Supplementary Table 10. Comparison of dry mass percentage of human and synthetic feces.

Organic Content	% dry mass – Human feces [14]	% dry mass – Synthetic feces
Bacterial biomass	25-54	43.33
Protein or nitrogenous matter	2-25	6.21
Carbohydrate or undigested plant matter	25	28.81
Fat	2-15	21.65

Supplementary Table 11. Physical parameters for the simulated toilet flushing systems.

Flow Rate (gpm)	1	1.5	2	2.5
Height (mm)	4.75	3.62	5.11	4.27
Re	4578	7136	9049	11632
Wall Shear (Pa)	0.093	0.33	0.28	0.60

Supplementary Table 12. Bacteria identification from mass spectrometry.

Organism (best match)	Score Value
Staphylococcus aureus	2.358
Enterobacter cloacae	2.281
Escherichia vulneris	2.256
Escherichia hermannii	2.212
Enterococcus mundtii	2.219
Acinetobacter calcoaceticus	2.077

Note: Any score value >2 indicates secure genus identification.

Supplementary Table 13. Impact parameters of synthetic feces on solid surfaces.

Solid Content Percentage (%)	Impact Area (m^2)	Impact Time (s)	Average Impact Force (N)
20	6.25×10^{-4}	6.45×10^{-2}	0.23
40	4.00×10^{-4}	1.30×10^{-2}	2.33
60	3.14×10^{-4}	5.00×10^{-3}	5.60

Supplementary References

1 Wang, J., Kato, K., Blois, A. P. & Wong, T.-S. Bioinspired Omniphobic Coatings with a Thermal Self-Repair Function on Industrial Materials. *ACS Applied Materials & Interfaces* **8**, 8265-8271 (2016).

2 Israelachvili, J. N. *Intermolecular and surface forces*. (Academic press, 2011).

3 Lewis, S. & Heaton, K. Stool form scale as a useful guide to intestinal transit time. *Scandinavian Journal of Gastroenterology* **32**, 920-924 (1997).

4 De Gennes, P.-G., Brochard-Wyart, F. & Quéré, D. *Capillarity and wetting phenomena: drops, bubbles, pearls, waves*. (Springer Science & Business Media, 2013).

5 Preston, D. J., Song, Y., Lu, Z., Antao, D. S. & Wang, E. N. Design of Lubricant Infused Surfaces. *ACS Applied Materials & Interfaces* **9**, 42383-42392 (2017).

6 Seah, M. P. An accurate and simple universal curve for the energy-dependent electron inelastic mean free path. *Surface and Interface Analysis* **44**, 497-503 (2012).

7 Lafuma, A. & Quéré, D. Superhydrophobic states. *Nature Materials* **2**, 457 (2003).

8 Semprebon, C., McHale, G. & Kusumaatmaja, H. Apparent contact angle and contact angle hysteresis on liquid infused surfaces. *Soft Matter* **13**, 101-110 (2017).

9 Kreder, M. J. *et al.* Film dynamics and lubricant depletion by droplets moving on lubricated surfaces. *Physical Review X* **8**, 031053 (2018).

10 McHale, G., Orme, B. V., Wells, G. G. & Ledesma-Aguilar, R. Apparent Contact Angles on Lubricant-Impregnated Surfaces/SLIPS: From Superhydrophobicity to Electrowetting. *Langmuir* **35**, 4197-4204 (2019).

11 Yunus, A. C. & Cimbala, J. M. Fluid mechanics fundamentals and applications. *International Edition, McGraw Hill Publication*, 185201 (2006).

12 Carson, C. A., Shear, B. L., Ellersieck, M. R. & Asfaw, A. Identification of fecal Escherichia colifrom humans and animals by ribotyping. *Appl. Environ. Microbiol.* **67**, 1503-1507 (2001).

13 Takahashi, M. K. *et al.* A low-cost paper-based synthetic biology platform for analyzing gut microbiota and host biomarkers. *Nature Communications* **9**, 3347 (2018).

14 Rose, C., Parker, A., Jefferson, B. & Cartmell, E. The characterization of feces and urine: a review of the literature to inform advanced treatment technology. *Critical Reviews in Environmental Science and Technology* **45**, 1827-1879 (2015).

15 Woolley, S., Cottingham, R., Pocock, J. & Buckley, C. Shear rheological properties of fresh human faeces with different moisture content. *Water SA* **40**, 273-276 (2014).

16 Woolley, S., Buckley, C., Pocock, J. & Foutch, G. Rheological modelling of fresh human faeces. *Journal of Water Sanitation and Hygiene for Development* **4**, 484-489 (2014).

17 Soheilian, M., Mazareei, M., Mohammadpour, M. & Rahmani, B. Comparison of silicon oil removal with various viscosities after complex retinal detachment surgery. *BMC ophthalmology* **6**, 21 (2006).

18 Jones, D. H. *et al.* Highly purified 1000‐cSt silicone oil for treatment of human immunodeficiency virus‐associated facial lipoatrophy: an open pilot trial. *Dermatologic Surgery* **30**, 1279-1286 (2004).

19 Patravale, V. & Mandawgade, S. Novel cosmetic delivery systems: an application update. *International Journal of Cosmetic Science* **30**, 19-33 (2008).

20 Council, G. S. Socio-economic evaluation of the global silicones industry. *Final Report* (2016).

21 Crisp, A., de Juan, E. & Tiedeman, J. Effect of silicone oil viscosity on emulsification. *Archives of Ophthalmology* **105**, 546-550 (1987).

22 Daniel, D., Timonen, J. V., Li, R., Velling, S. J. & Aizenberg, J. Oleoplaning droplets on lubricated surfaces. *Nature Physics* **13**, 1020 (2017).